# Cold Working Holes in Multi-Layer Members

Kevin Bryan Connolly

Dissertation paper submitted to the faculty of the Virginia Polytechnic Institute and State University in partial fulfillment of the requirements for the degree of

Doctor of Philosophy

In

Engineering Mechanics

Norman E. Dowling (Chair),

John C. Duke,

Rakesh K. Kapania,

Shane D. Ross,

Surot Thangjitham

September 9, 2014

Blacksburg, Virginia

Keywords: cold expansion, finite element, simultaneous expansion

# Cold Working Holes in Multi-Layer Members

Kevin Bryan Connolly

## Abstract

Increasing the life cycle of critical components is a common goal in many vehicle industries. One of the most common ways to increase the fatigue resistance of fasteners holes is the process of cold expansion. This method introduces a compressive stress field in the region around the hole that slows the propagation of cracks. Determining the life cycle benefits gained from cold expansion is difficult due to the complex nature of the residual stress field. Many groups have attempted to accurately predict how this field is generated and what factors can cause major variations in the resulting stress field. There are still many factors related to the cold expansion process that have not been quantified. By creating a script in the computer language Python it was possible to generate a number of different models quickly and efficiently in the finite element program Abaqus. While not all the models that could be created were initially found to be convergent, the script proved useful in creating a varied number of models to assist in determining which factors were leading to the convergence problems. Confidence in the script's ability to produce accurate models was established by generating models that mirrored the conditions found in other literature, so that a direct comparison of results could be made. For this work two factors were considered for analysis, the effect of starting hole size and multi-layer expansion. The results showed that even within the range of recommended starting hole sizes, a difference in the residual stress field was evident. If the hole was expanded beyond the recommended size a threshold was reached and a severe weakening of the residual stress field was noticed. In the case of two plate expansion, changes in the residual stress field were only observed at the interface region of the plates. For the entrance face of the second plate in the expansion, this change was highly beneficial. The results from the two plate expansion suggest that artificially creating a multi-layer stack-up may be a useful tool to improve the residual stress field at the entrance surface of a plate

# Table of Contents

# Table of Figures

# Table of Tables

# 1 Introduction

Fleet maintenance is a vital component of the aircraft industry. The inspection and repair of essential components keep aircraft safe until they are eventually retired. The process of scheduling down time, pulling from service, performing inspections, executing repairs, and getting back into operation is costly. Not only is there a monetary cost associated with parts and man hours required to complete the service but also an opportunity cost accumulated during the time the aircraft is down.

Design techniques are used so that the failure path of the aircraft is known and inspection areas can be specified. Determining the failure path involves understanding which components in an aircraft will degrade faster. The safeties in place ensure that the aircraft does not risk a catastrophic failure; these include both redundancies in the design as well as scheduled inspection and maintenance [Tiffany, 2010]. As discussed before, downtime is expensive and therefore planned so that the aircraft is kept safe without being overly conservative.

It is now known that specific areas on an aircraft tend to accumulate damage faster than others. Material behavior studies have been used to determine where the highest risk areas exist. Risk factors can be caused by both environmental and design factors. A component exposed to high heat, harsh environment, or both can erode or become brittle, decreasing its ability to function. Structural material in the vicinity of stress raisers experience higher stresses than the surrounding area making them more prone to yielding, brittle failure, and fatigue. Common stress raisers on an aircraft include joints, fastener holes, and material cut outs. If multiple stress raisers are present within close proximity then there can be a compounding effect.

In an effort to improve safety, different methods have been employed to extend the life of components in high damage locations. These techniques include surface treatments that help fight corrosion and strategies for increasing the performance of components prone to high stress. One method to improve the life of components subject to fatigue is the process of cold work. In this method a material is exposed to a high local stress that yields the surrounding material. Upon removal of this stress the plastically deformed area is compressed by the elastic region beyond, leading to a compressive residual stress state. The compressive residual stress field slows the growth of cracks by effectively lowering the maximum stress seen by a crack tip in this region. Of particular interest for this work is the cold working of fastener holes, usually termed cold

expansion (CX). In this process a ball or mandrel is pulled through the hole, plastically deforming the annular region around the hole. The compressive residual stress that results from this process slows the growth of cracks emanating from the hole.

Cold expansion is most commonly used with fastener holes such as those for bolts and rivets. Today it is common for manufacturers to cold work components during aircraft construction and maintenance. While it is accepted that this process improves the fatigue life of components, its application is not considered when determining the maintenance cycle for the aircraft. To be taken as a credit towards the maintenance cycle, both the residual stress field produced by the cold expansion and its effect on the fatigue life of components must be well characterized.

Before the fatigue life can be determined, it is essential that the residual stress field produced by cold expansion is understood. To achieve this goal groups have used a variety of analysis tools to determine the important characteristics of the cold work process and precisely how it affects fatigue cracking. Among the methods used are analytic models as well as numeric simulation. To fully understand the cold expansion process a number of geometric and environmental variables have been explored. However, in all studies important aspects of real structures have been ignored to reduce the number of variables. The purpose of this work is to explore the effect of multi-layer cold expansion as well as the effect of hole size on the residual stress field.

# 2 Background

During the early period of commercial flight, a series of fatal plane crashes caused investigations into the mechanisms that can lead to failure. Analysis found that these aircraft failures were due to fatigue caused by the cyclic pressurizing of the hull. After further investigation of wreckage and the testing of aircraft pulled from service, it was found that the fatigue cracks were initiating at fastener holes in the vicinity of fuselage cut outs made for the aircraft's square windows [Smith, 1986]. These incidents launched research into how stress concentrations affect the fatigue life of components on aircraft. This also started interest in redundancy methods and other techniques to extend component life in critical areas with a minimum of additional weight.

Bolts and rivets are used extensively in a number of industries including the aircraft industry. They can be more convenient than welding and allow pieces to be separated at a later date. This can allow components to be removed and replaced with less time and difficulty. However, these holes along with other geometric discontinuities will cause locally higher stresses. The area around these stress raisers will be more prone to fatigue damage as it will experience higher peak stresses during cyclic loading [Dowling, 2013]. The exact magnitude of a stress raiser depends on the geometry and has been calculated analytically for a many simple cases. More complex interactions are generally analyzed using finite element methods.

The area around these fastener holes can be strengthened using cold working techniques. Cold working is the process of permanently deforming material at room temperature to modify the materials characteristics. In the case of fastener holes, the cold working process is used to plastically deform the area around the hole and create a compressive residual stress field. The cold working of fastener holes, commonly done by cold expansion (CX), has been used since the 1960’s [Reese, 2009]. This method involves pulling an oversized ball or mandrel though the fastener hole, with some techniques using a sleeve so there is no direct contact between the ball/mandrel and the hole surface. In this method, the forced expansion of the material at both the hole surface and along the bore causes yielding and a plastically deformed area. The elastic material beyond the plastic strain region, in trying to return to its original, zero stress, zero strain, position, puts the plastically deformed region into a compressive stress state. This is illustrated in Figure 2.1.

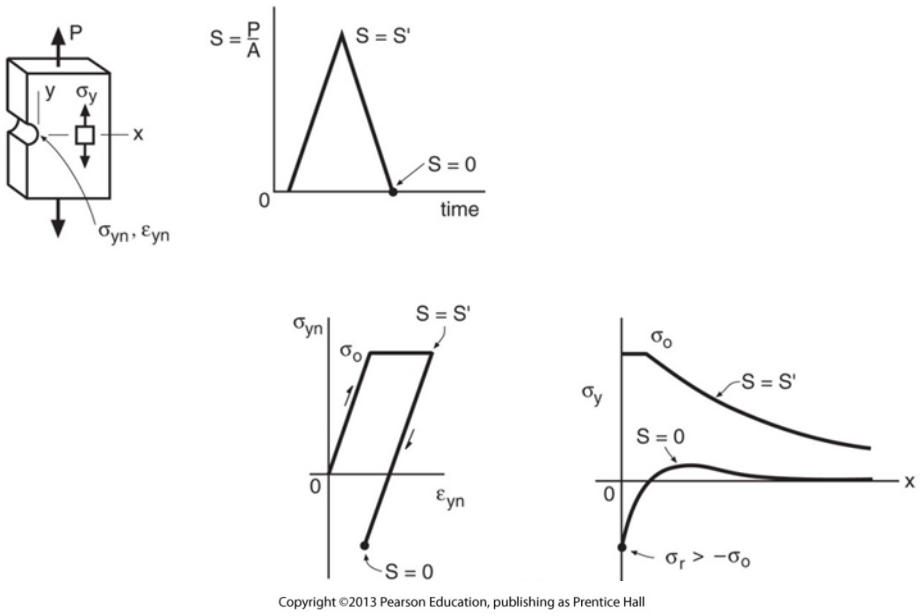


Figure 2.1: Stresses during loading and unloading with local plastic deformation at a stress raiser [Dowling, 2013 p.523].

To determine the benefits of the cold expansion process it must be assessed in terms that are used for general fatigue analysis. In the field of fracture mechanics the severity of a crack is characterized by using the concept of the stress intensity factor, *K*. This factor is defined as a function of the applied stress, *S*, a geometric factor, *F*, and the crack length, *a*.

$$K = FS\sqrt{\pi a}$$

The geometry factor is an analytically determined value used to relate the size of the crack to the shape of the component in which it exists. This factor is based on the crack situation, seen in Figure 2.2, as well as the ratio between crack length and component width, *a*/*b*, $F = F(geometry, a/b)$. The value of the geometry factor will change as the crack grows. For sufficiently short cracks a single value may be used, while complex equations can be used to estimate the value for larger cracks.

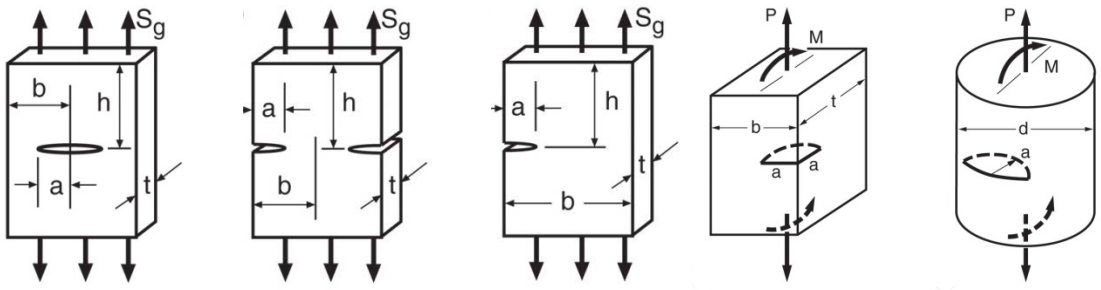


Figure 2.2: Basic crack geometries.

In the calculation of fatigue life the applied stress range is used to calculate the stress intensity range experienced at the crack tip. The stress intensity range ,$\Delta K$, is then used to make estimations for the crack growth rate, $\frac{da}{dN}$, in a material, example test data shown in Figure 2.3. Such calculation must be made carefully as both the crack length and geometry factor are changing with each cycle.

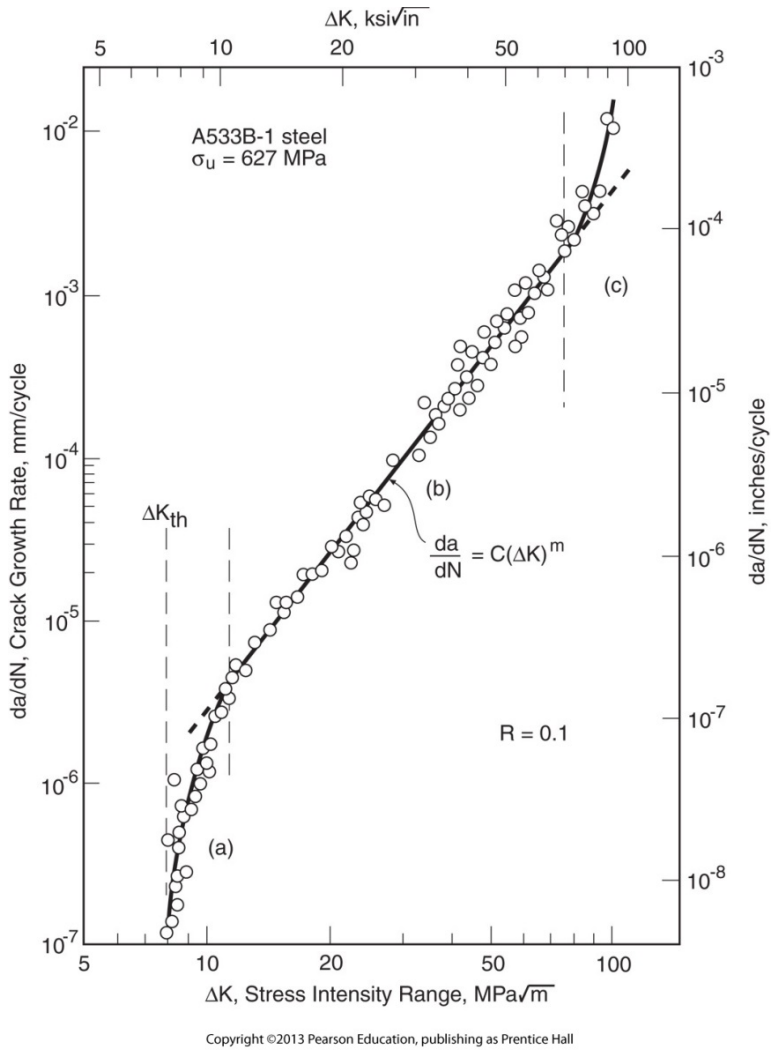


Figure 2.3: Example $\frac{da}{dN}$ vs $\Delta K$ graph for a ductile pressure vessel steel [Dowling, 2013 p.547].

The compressive residual stress is able to impede crack growth by effectively reducing the stress intensity factor in the region of the residual stress field. It does this by effectively lowering the applied stress, *S*. Studies have shown that the compressive residual stress field primarily increases the growth portion of a crack's life [Lacarac 2000]. The time to crack initiation has shown either a small or detrimental effect from cold expansion. The cold expansion process can damage the hole providing sites for early crack initiation. For this reason, sleeves are generally used to reduce the damage that can be caused. It has been demonstrated that this damage along with poor reaming can severely limit or negate the benefits to the total fatigue life [Clark, 2003].

A common form of cold expansion among both civilian and military aircraft industries is the split sleeve method, shown in Figure 2.4. This technique was standardized by Boeing, the first company to use a significant amount of cold expansion during the production of their aircraft [FTI, 2011]. Before this, cold expansion had been used to extend the life of aircraft that had already seen some amount of service and was not a well-controlled process. Fatigue Technology Incorporated (FTI), once part of Boeing but now a separate company, handles cold expansion for many aerospace groups. Their flagship cold expansion process uses a number of well controlled steps. First, a rod attached to the mandrel is fitted through the nosecap into a pneumatic puller. The sleeve, a circular tube cut along its length, is then placed over the mandrel and slid down the rod until it is seated on the nose cap. It should be noted that without the additional thickness of the sleeve the mandrel can pass through the hole. Once the components are in place, the mandrel is fitted through the hole so that the plate also rests on the nosecap and the sleeve is seated inside the hole. The pneumatic puller is then used to draw the mandrel through the hole, yielding the plate and the sleeve. The side of the plate that the mandrel enters will be referred to as the entrance surface while the reverse is the exit surface. The expansion applied to aluminum and mild steel alloys range from three to six percent of the initial hole diameter, while titanium and high-strength steel are expanded by 4.5 to 6.7 percent [FTI, 2011]. During the expansion process, the split in the sleeve allows it to open while the bottom of the sleeve is supported by the nosecap. The split sleeve is lubricated on the inside and allows the mandrel to be pulled through while generating less shear stress on the hole. This means that there is less material being pulled along the bore of the hole and should allow for lower through thickness variation in the residual stress field. This process causes a high amount of deformation to occur at the split in the sleeve; this region is called the pip. In order to avoid problems caused by this non-uniformity, components are generally cold expanded so that the pip occurs at the top of the hole, where the top/bottom axis of the hole is in line with the stresses that will be applied. In most cases, reaming is used after cold expansion to remove damaged material and ensure that the hole is circular and the correct diameter.

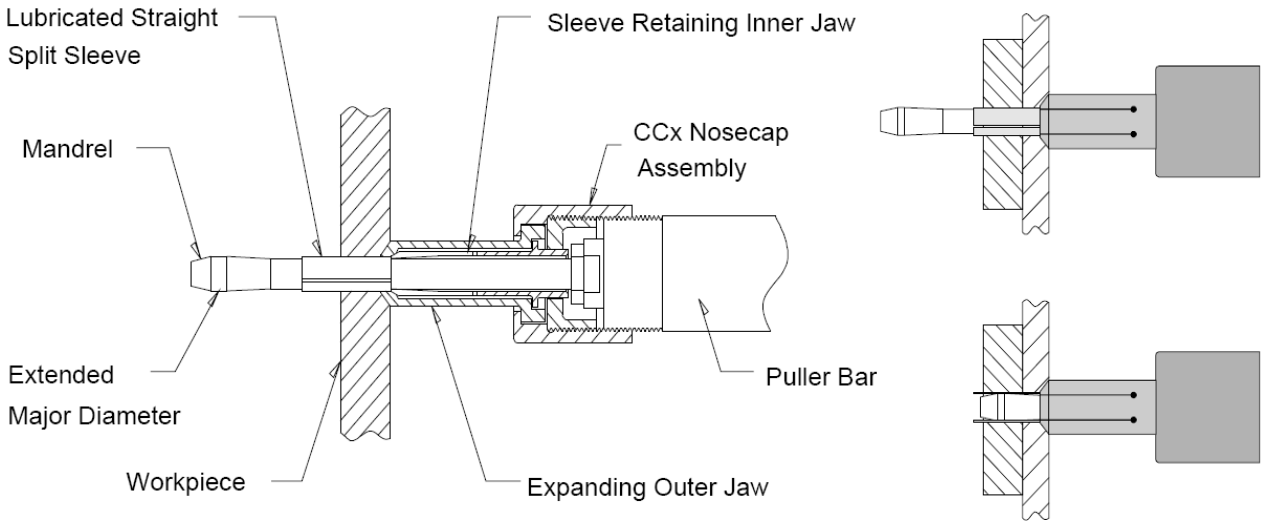


Figure 2.4: Diagram of split sleeve cold expansion [FTI, 2011].

FTI has developed different tool sets to be used depending on the initial hole size and the material of the plate. The split sleeve expansion retailed by FTI is popular due to two advantages: (1) Due to the sleeve, this technique results in less damage to the material around the hole. (2) The method can be performed with access to only one side of the hole, which is crucial for cold expansion of assembled aircraft when one side of a hole is inaccessible.

# 3 Literature Review

Cold expansion is applied to both new and in service aircraft as a basic means of life extension. It is generally accepted that this process can extend the fatigue life of the component by two to ten times its normal life [Reid, 2001]. This effect shows lower life improvement at higher stress levels and greater life improvement at lower stress levels. The level of improvement for an arbitrary case has proven difficult to quantify.

Groups have tried different methods to account for the effects of cold expansion. In most cases the residual stress field was taken into account by modifying the stress intensity factor to make life predictions. A technique used by [de Matos, 2007] utilized crack growth data to determine this modified stress intensity factor. After conducting fatigue experiments at different stress levels with both cold expanded and non-expanded specimen, crack growth data was collected using a scanning electron microscope (SEM). This data along with fracture mechanics techniques were used to make calculations that matched the predicted results [de Matos, 2007]. Another method implemented by [Lacarac, 2000] used the remote opening stress to calculate a modified stress intensity factor at the crack tip, in the presence of the residual stress field. Optical techniques (microscopes and cameras) were used to determine the remote applied stress at which the crack face was fully open. This opening stress was used to calculate a stress range, used in the calculation of a modified stress intensity range. During testing replica techniques were used to determine how the shape of the crack was changing. Based on whether or not the crack went through the thickness, different geometric factors were used to make the calculation. It was seen that this method worked well for calculating crack growth in both plain and cold expanded specimens. However, this was only true when the crack geometry was known and the appropriate geometry factor was used during the calculation. The techniques used in these papers worked well, but required detailed measurements over the life of the test specimen. While the predictive abilities of these studies were limited, they did show that data could be matched using a modified stress intensity factor.

In order to take credit for the benefits of cold expansion, there must be a capability to make life predictions across a variety of components and situations without testing all specific cases. To accomplish this goal, work has been conducted to understand the factors that contribute to the residual stress field and how it interacts with cracks to make stress intensity predictions.

Different modeling schemes have been used to predict the residual stress field produced, given the material properties, component geometry, and degree of cold expansion. These estimates were usually compared to measurement taken from test specimens.

The most common way to measure residual stresses is the use of non-destructive x-ray diffraction. This method, however, can only measure the surface layer, $\approx 20$ μm [Noyan, 1987], making it limited for analyzing cold expansion, because the residual stress field varies through the thickness of the material. In addition to only being able to take surface measurement, x-ray diffraction is also limited by the fact that it cannot measure point stresses and must average the stress over the size of the beam, a square area 0.5 mm to 13 mm on a side [Prevey, 1986]. In the case of the residual stress field produced by cold expansion, the stresses changes very rapidly close to the hole and averaged measurements make interpreting data difficult. Another technique used for measuring residual stresses is neutron diffraction. This operates in a similar manner to x-ray diffraction and is also limited by the averaging of stresses on the order of 1-2mm [Noyan, 1987], however, it can be used to take measurements at different depths through the material. Two newer non-destructive methods, photon induced positron annihilation and meandering winding magnetometer arrays, have also shown promising results in their capability to measure residual stresses [Ball, 2003].

A new destructive method called the Garcia-Sachs method can be used to determine the average through thickness residual stresses left by the cold expansion [Garcia-Granada, 2001]. This method involves placing strain gages radially around a cold worked hole, then removing small amounts of the hole at a time, and measuring the change in the strain [Lacarac, 2004]. The averaged through thickness measurements can then be made at an accurately defined radius. The disadvantage of this system is that only an average though thickness stress can be measured, specimens must be circular, and further testing cannot be done on the specimen after measurements are made. Another destructive technique, the contour method, is capable of measuring the residual stress field through the thickness of a component on a chosen plane [Ismonov, 2009a]. In this method, the specimen is cut along a plane and the minute deformations along the newly freed surface are measured. These surface displacements are used with a finite element simulation to estimate the residual stresses acting on that plane to create the observed deformation field.

Initial attempts to model the residual stress field included the development of analytic methods [de Matos, 2007; Lacarac, 2000]. Due to the free surfaces at the entrance and exit faces of the component with constrained material between them, there is a significant through thickness variation in the residual stresses. Purely mathematical models generally produce poor results because the small strain assumption cannot be used for studying cold expansion and fracture mechanics models can only be used to estimate the average stress through a plate [Chakherlou, 2003]. For these reasons, numeric models are more frequently used. Two-dimensional models cannot capture the three-dimensional nature of the residual stress field and are therefore rarely implemented. In-plane, two-dimensional models are only capable of generating an average stress at a given radius. While axisymmetric models could estimate the through thickness variation, they cannot account for different boundary conditions on the component. Through experimentation and observation it has been seen that the average stress through the plate is less useful for estimating the stress intensity factor. It has been shown multiple times, [Lacarac, 2000], that the intensity of the residual stress field is lower at the surfaces where the material is not constrained. Additionally the entrance surface has consistently shown lower stresses than the exit surface. This leads to early crack propagation consistently occurring at the entry surface of plates. In addition to early crack propagation occurring at the lower stress entrance surface, cracks have been seen to begin propagation through the thickness only after the surface crack has reached past the zone of maximum compressive stress [Clark, 2003]. This gives the crack an odd shape and also makes it difficult to predict when through crack mathematical models can be used, Figure 3.1.

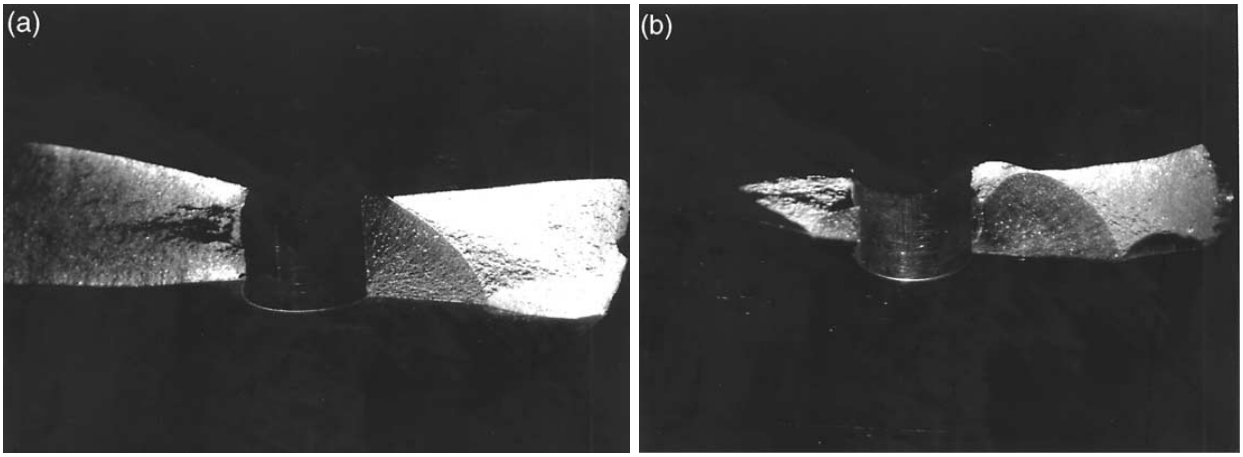


Figure 3.1: (a) Non-expanded hole crack profile. (b) A typical expanded hole crack profile [Clark, 2003].

It has been shown that even if the stress intensity factor is measured from experiments, but the geometry of the crack is not known, then crack growth predictions are not accurate [Lacarac, 2000]. These experiments further emphasize the need for fully three-dimensional analysis of the residual stress field in order to make accurate life predictions.

Finite element tools have allowed the modeling of both simple and complex aspects of split sleeve cold expansion. Early models employed a simplified expansion process, using the application of uniform pressure or displacement to expand the bore of the hole. These simplifications did show differences in the residual stress field through the thickness, but results at the entrance and exit surfaces did not match measurements taken using X-ray diffraction. These expansion models produced identical stresses at both the entrance and exit surfaces, while experimentation has shown that the exit surface has a higher residual stress than the entrance surface. Later models incorporated the use of the mandrel in simulations and were able to achieve the proper residual stress phenomenon. Models have been created for both ball and tapered mandrels. Most of the available literature features tapered mandrels as these are more common in field work. As finite element software advances, it becomes possible to create more complex models that include more parts and better represent the interaction between them. In recent years models have been made that include both the sleeve and mandrel to simulate cold expansion. The addition of the sleeve alone did not considerably change the residual stress field produced during cold expansion [Ismonov, 2009a]. However, if the sleeve is allowed to have an opening as in split sleeve cold expansion, then the residual stress around the split is dramatically changed [Ismonov, 2009a; Houghton, 2011]. The use of the sleeve also affects how friction can change the residual stress field. Adding friction effects to the cold expansion process does not significantly change the majority of the residual stress field but it has been shown to have an effect on the entrance surface of the hole [Houghton, 2011]. This is important, because, as mentioned previously, the entrance face is generally the site where the crack begins to propagate, and any changes to the residual stress field in this area are important to recognize.

Additional effects considered in past work are those that occur while the component is in use. For example, different analyses have been conducted on the behavior of the residual stress field itself. These included common elements experienced by cold worked holes in the field. Some of these factors included raised temperatures [Clark, 2003; Lacarac, 2001], cyclic overloads, both tensile and compressive [Toor, 1976; Callinan, 2010], and friction [Ismonov,

2009a; Houghton, 2011]. Further work has been conducted to analyze specific cases of interest. Other examples include how a cold worked hole performs as part of a lap joint [Ismonov, 2009b; Chakherlou, 2012], performance of a cold expanded hole with a bolt in place [Chakherlou, 2011; Cook, 1989], and the residual stress field created if a hole is cold expanded twice, by pulling the mandrel through in both directions [Stefanescu, 2003]. However, these models performed the cold expansion process only on a single plate. In reality, this process is usually carried out on components that are comprised of at least two layers. Since fasteners in aircraft are used to connect different portions together, and to ensure they fit together properly, multiple plates are cold expanded simultaneously. This simultaneous expansion is only consider in [Finney, 1995] where an attempt is made to experimentally quantify the effect of multi-layer cold expansion. This work also considers the effect of interference fasteners and how it can affect fatigue life. In has been shown in bolt tightening experiments that additional constraints on the hole can affect the residual stress field. This is predominantly true where there is out of plane displacement as seen at the hole edge [Chakherlou, 2011; Finney, 1995]. No previous numeric analysis is known that examined the cold expansion of more than one layer.

# 4 Research Objectives and Methods

Previous work has shown that the entrance surface of a cold expanded plate is extremely important when examining the life improvement potential of cold expansion. Through experiments, it is known that the corner of the plate at the entrance surface of the hole is consistently part of early crack propagation. This crack behavior is in line with the understanding of the residual stress field produced by cold expansion. With a weaker residual compressive stress, cracks starting at the hole edge will naturally grow faster in this region, leading to consistent early crack growth.

With the entrance surface of the cold expanded hole playing such a crucial role, it is important to take into account any factors that could influence the residual stress in this region or reduce the magnitude of the residual stress field in another region. This work will examine factors not previously considered in the literature. The first will be the effect of hole size variation on the residual stress field. FTI has stipulated acceptable hole size ranges for proper uses of each tool set. This work will examine how the residual stress field changes between the maximum and minimum tolerance values as well as some hole sizes outside the tolerance. Second, the modeling of multi-layer cold expansion will be examined. It has been seen in studies that stresses applied at the hole surfaces for cold worked holes can affect the stress through the thickness. This is particularly true at surfaces where out of plane displacement has occurred. When cold expanding a multi-layer member, the exit surface of one plate will be pushed against the entrance surface of the next plate. With both plates experiencing out of plate displacement, it has never been shown how the residual stresses will be affected. The final variation that has not been explored is the effect of a counter-sink at the exit hole. In the aircraft industry, cold expansion is frequently used on the holes that connect the skin of the wing to underlying structural members. Holes machined with counter-sinks are commonly used with the skin so bolts will be flush and aerodynamics will be unaffected. The angled slope of the counter-sink means that some of the expansion stress will not be fully transferred to the hole, resulting in a reduced residual stress. As none of these situations have been explored in the literature, experimentally or using finite element simulations, it will be important to identify whether these effects can change the location most conducive for crack propagation.

While the insights gained by complex models are useful, it comes at the cost of simulations that are more difficult to create and take longer to run. Depending on the end use of the simulation, certain aspects of the most complex model may not be needed. In addition to examining different cold expansion parameters, an additional focus of this work is to create a model that will be robust enough to handle a number of parameters interchangeably. Along with being able to handle different specifications related to the reality of the cold work situation, this model will be able to handle variations in the geometry as well. This kind of model would allow for easy comparison between different situations. Variations could include the effects of plate thickness, varying the counter sunk depth, using different mandrel sizing, changing material, and other factors.

This model flexibility will be accomplished by using script to generate the model. This script, written in Python, will generate the model as described by parameters defined at the outset of the script run. Parameters that could change from model to model include hole size, plate thickness, plate width, plate material, number of plates, and other basic values used to define the model. Along with a check box system to include aspects such as friction, sleeve split, presence of a counter sink, and other functions, the script will allow for a large range of models to be produced. As long as the model is robust enough, this method will allow the creation of different models quickly and consistently. Using another script file, data can be extracted from the model in areas of interest. These scripts will allow model generation and data gathering to occur in a quick and repeatable fashion. This will make it possible to examine how factors such as oversized holes, thin plates, and material stack-ups can affect the residual stress field. The end product of this work, to be completed in the future, is to create a residual stress database for common component geometries seen in aircraft. These residual stress fields may be used with multi-dimensional crack propagation tools to make life predictions for standard cases.

As this kind of study has not been done before it will be difficult to assess the accuracy of these models. The convergence of the model itself will be checked by making small changes to the mesh and surface interactions to confirm that these changes do not radically affect the output. To test model accuracy, the script will be used to generate models similar to those described in existing literature, so that outputs can be compared [Houghton, 2011, Ismonov 2009a]. For those papers that have test results, the model will also be compared to these [Ismonov 2009a].

While the model should be robust enough to handle the variations described above, it will also be important to examine the degree to which particular variations affect the model output. The purpose is to determine an optimal configuration in which the model is as simple as possible without compromising its accuracy. By running models with and without a particular factor, such as friction, it will be possible to find the effect on the output and determine under what circumstances it should be included in future modeling. Making the model simpler will reduce the time it takes to run and decrease the number of constants needed to create the model.

# 5 Modeling

The majority of time spent on this project has been devoted to creating the finite element models used in this study. For this work, the commercial finite element software Abaqus was used. The computer language, Python, is used in the background of the Abaqus graphic user interface (CAE), therefore it was chosen to write the script used to interact with the software. The first goal of this project was to determine the parameters for a “baseline” model that would be used to draw comparisons between different model variations. The inspiration for this project was a two layer cold expansion, consisting of a wing spar made of Al 7075 and a wing skin of Al 2024, both with a hole sized for quarter inch cold expansion. The materials, dimensions, and hole size for this situation were taken from what might be found at an aircraft wing fastener hole to connect the wing skin to wing spar.

## 5.1 Component Dimensions

The “baseline” model was dimensioned after the Al 7075 plate from the previously mentioned stack-up. This was done so it could be used directly in later analyses. A diagram with the dimensions for the modeled plate is given in Figure 5.1. The width of the plate was chosen based on the hole to edge distances used for previously manufactured cold expansion test specimens. A decision was made to make the plate section square, so that changing boundary conditions could be accomplished with fewer issues. It was only necessary to model half the plate by implementing symmetry conditions. The plate was created by defining the cross-section and extruding it to the appropriate thickness. Prefixes of H or V, seen in the Figure 5.1 though Figure 5.3, denote that the distance is measured along the horizontal or vertical axis respectively.

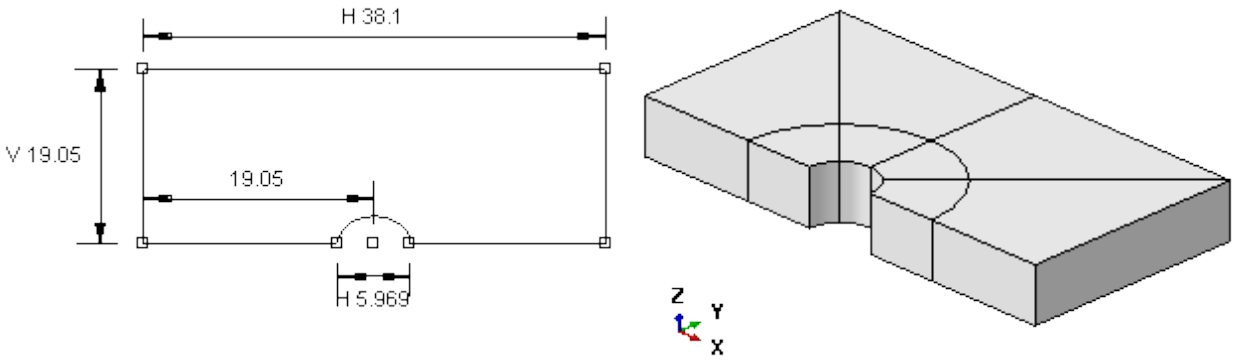


Figure 5.1: Dimensions for the "baseline" plate cross-section, given in mm (left) and modeled component produced buy extruding the cross-section 6.88mm (right).

In addition to the plate, the "baseline" model also consists of the sleeve and mandrel required for cold expansion. The sleeve width, or thickness, was taken directly from FTI regulations, while the sleeve height was dimensioned so it would have the minimum required clearance. Like the plate, symmetry conditions were used and only half of the sleeve and mandrel were modeled. The sleeve was created by dimensioning the cross-section and revolving it around the sleeve center. The sleeve cross-section and model are shown in Figure 5.2.

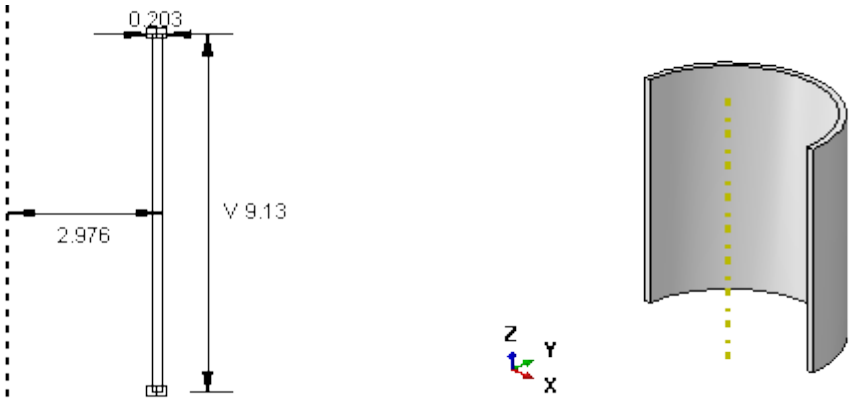


Figure 5.2: Cross-section dimensions for sleeve, given in mm (left) and modeled component produced by revolution (right).

The dimensions for the mandrel consist of the minimum and maximum values for the diameter and the lengths for each section of the mandrel. The mandrel diameters are given in the user's manual, but the section lengths were estimated from images and crude measurements on the tool. Like the sleeve, the mandrel was also produced by revolution. However, instead of using a cross-section, only the outside surface of the mandrel was used to create the part, shown in Figure 5.3. The rod connected to the mandrel would attach at the bottom, making the more

gently sloping surface the first to enter the plate. The dimensions used to design all components for the “baseline” model can be found in Table 5.1.

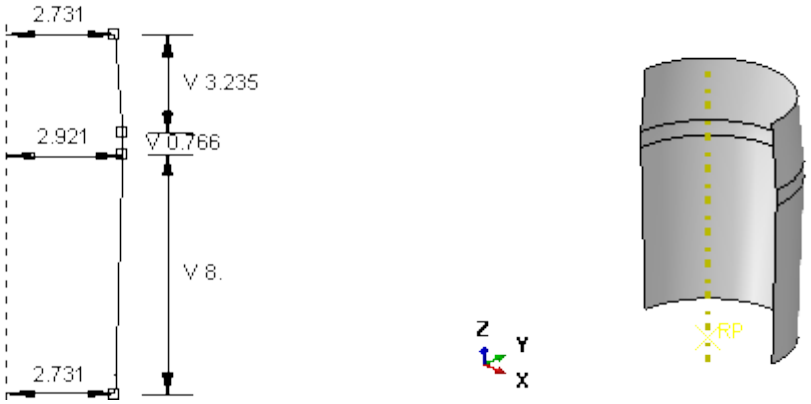


Figure 5.3: Ouside dimensions for madrel, given in mm (left) and modeled component produced by revolution (right).

Table 5.1: Dimensions used to create baseline model.

| Component Dimensions | Value |
|---|---|
| Half Plate | |
| Length ($L$) | 38.100 mm |
| Width ($W$) | 38.100 mm |
| Hole Diameter ($D$) | 5.969 mm |
| Thickness ($t$) | 6.880 mm |
| Sleeve | |
| Width ($w$) | 0.203 mm |
| Potential Half Sleeve Opening ($\phi$), degees | 0.5° |
| Outer Diameter ($d_o$) | 5.952 mm $= \left(D\,\frac{180-\phi}{180}\right)$ |
| Height ($h$) | 9.130 mm $= \left(t + 3(0.75)\right)$ |
| Mandrel | |
| Minor Diameter ($Mi$) | 5.461 mm |
| Major Diameter ($Ma$) | 5.842 mm |
| Entrance Length ($S1$) | 8.000 mm |
| Middle Length ($S2$) | 0.766 mm |
| Exit Length ($S3$) | 3.234 mm |

## 5.2 Coordinate Systems and Assembly

In all models, the plate(s) are positioned to rest in the *x*-*y* plane, while the mandrel moves along the *z*-axis in the –*z* direction. Coordinate systems are established with the datum located at the center of the hole on the exit surface. The coordinate systems used and datum locations are illustrated in Figure 5.4. For the analysis of models, different positions through the plate will be referred to by their percentage of the thickness away from the *x*-*y* plane. For instance, positions located at the exit surface will be referred to using $z = 0.0t$, the mid-thickess $z = 0.5t$, and the entrance surface $z = 1.0t$. When two-plates are expanded simultaneously in the field, it is the interior component that is expanded first. For the wing connection examined here, it is the structural spar, made from Al 7075, which is expanded first and becomes the top plate in the simultaneous expansion. Figure 5.5 illustrates the positioning of plates in a two-plate model along with the datum location and position references.

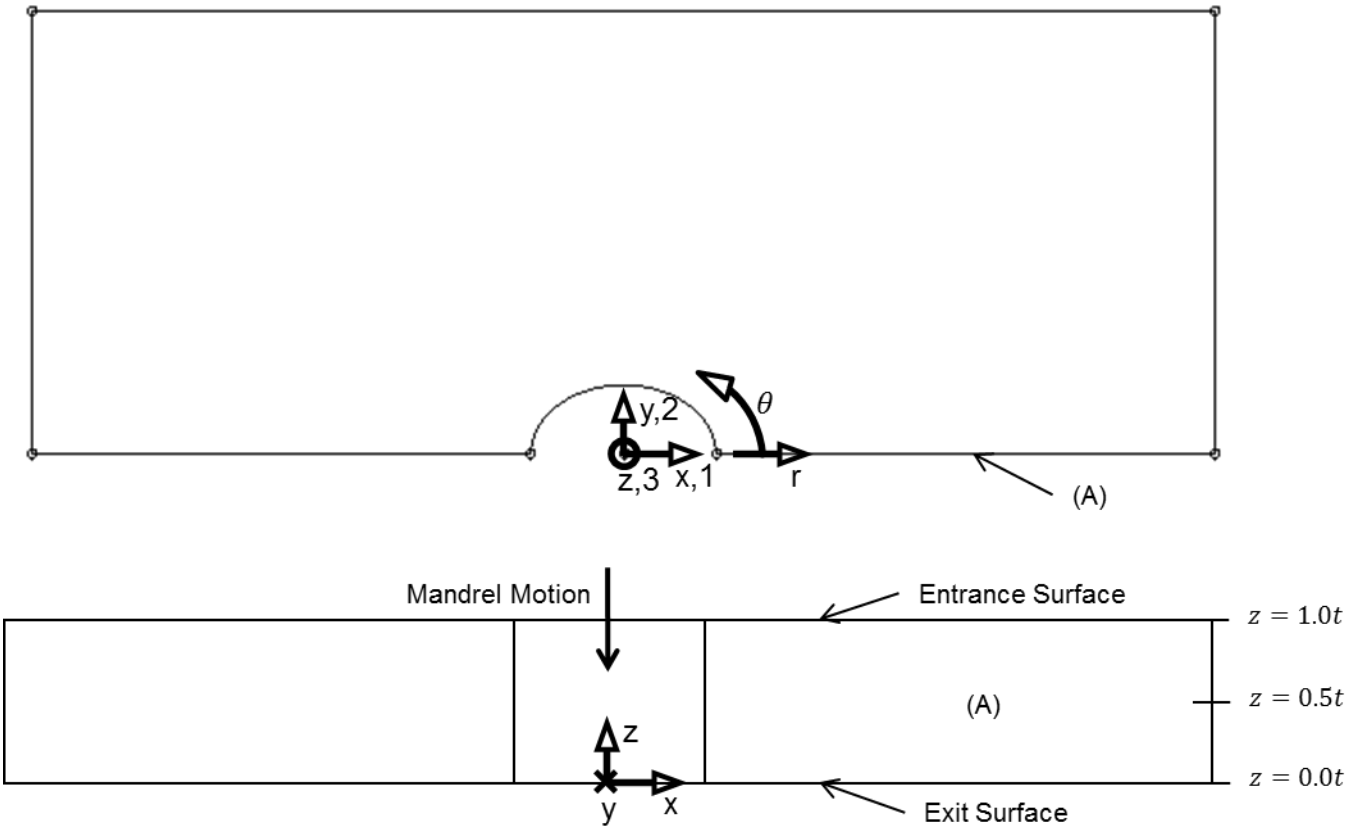


Figure 5.4: Orthographic representation of the coordinate system and datum configuration for a single plate model. Results given later for surface (A).

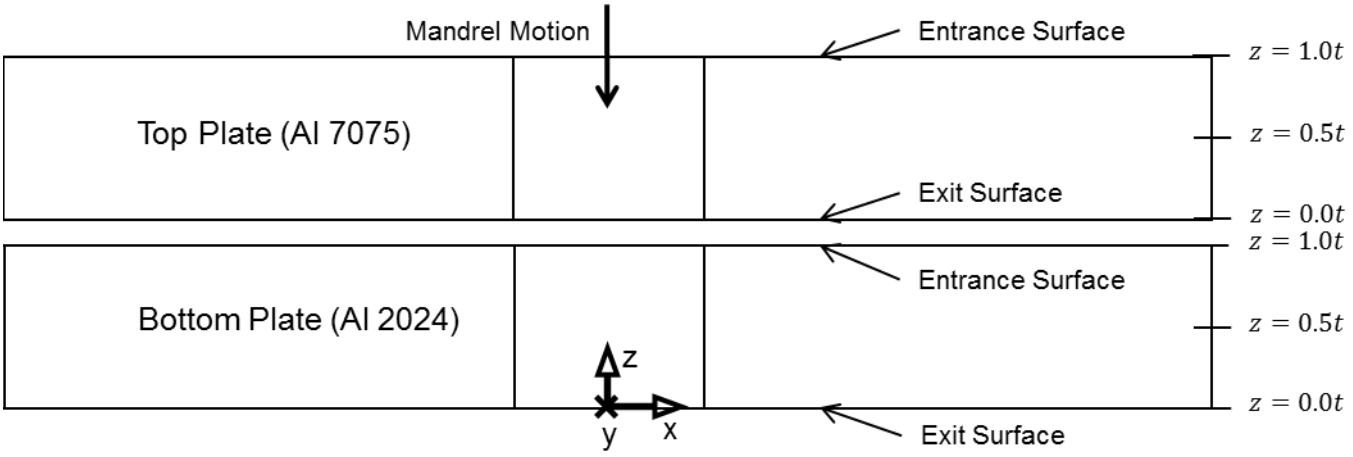


Figure 5.5: Illustration of the two-plate configuration and notation.

Model components were constrained using a number of boundary conditions. Fully fixed requirements were applied at the ends of plates, *y*-symmetry conditions along the *x*-z plane, and

*z*-fixed boundary condition at the bottom of the sleeve. These boundary conditions are shown for the single plate model assembly in Figure 5.6. Constraints on the mandrel prevent rotation and movement except in the *z*-direction, which was specified to accomplish expansion. Figure 5.7 illustrates how the modeled section fits into the component as a whole.

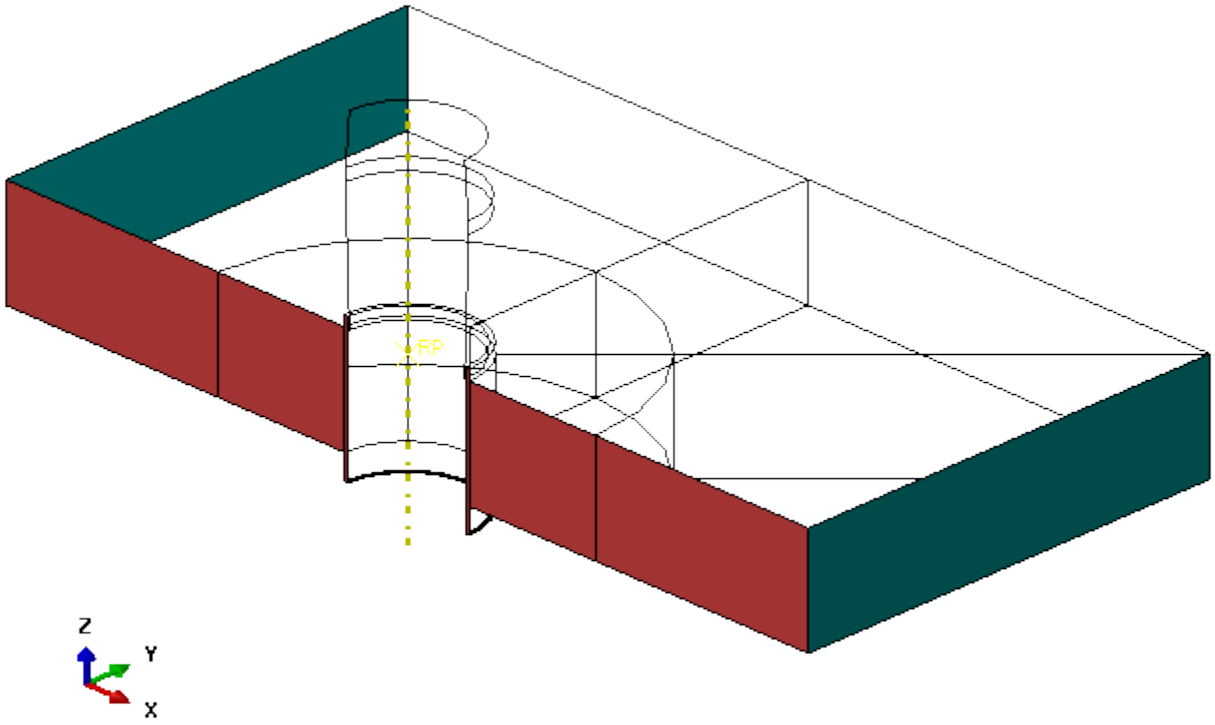


Figure 5.6: Assembly of "baseline model" showing boundary conditions, *y*-symmetry as red, full fix as green, *z*-fixed as black.

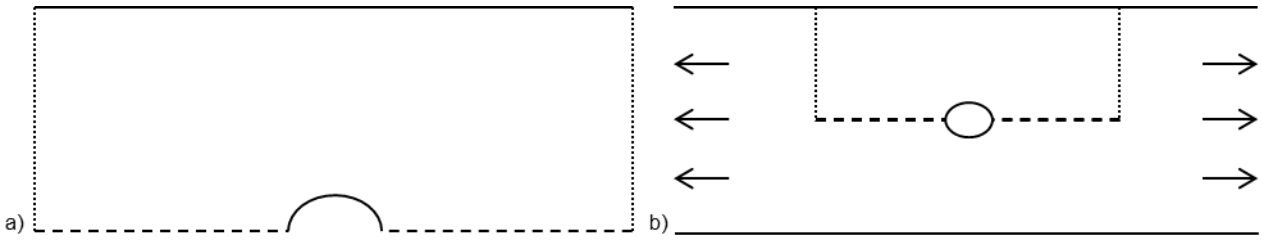


Figure 5.7: (a) 2D representation of boundary conditions, symmetry condition shown using dashes and fixed condition using dots, (b) illustration of modeled section with respect to component.

## 5.3 Material Properties

The plate material for all cases was defined using a plastic kinematic hardening model. The kinematic model was chosen over an isotropic model due to the nature of aluminum and

how it behaves in cases of reverse yielding. The properties of the plate materials used are described in a bilinear form. The stress strain curves for the 7075 and 2024 aluminum, along with their bilinear approximations, are given in Figure 5.8. The sleeve was modeled as being a fully elastic tool steel. The fully elastic assumption was used because the residual stresses in the sleeve are not important for this study. The mandrel and nosecap, made of hardened steel, are modeled as rigid to simplify the model. The elastic material properties for the sleeve and plate components are given in Table 5.2.

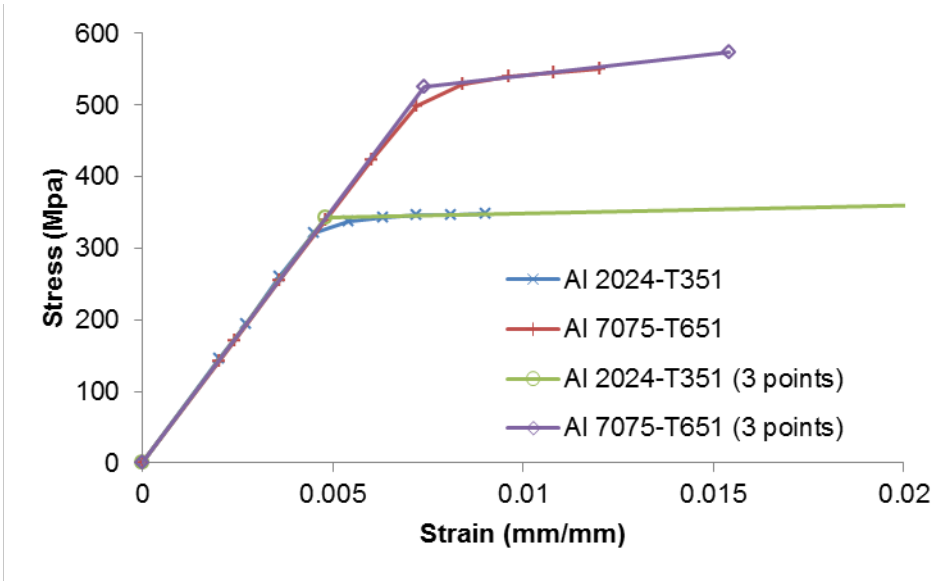


Figure 5.8: Stress vs strain curves used to define Al 2024 and Al 7075.

Table 5.2: Elastic material properties used for modeling.

| Material Property | Value |
|---|---|
| Al 2024 | |
| Elastic Modulus ($E$) | 73.1, MPa |
| Poisson's Ratio ($\nu$) | 0.33 |
| Al 7075 | |
| Elastic Modulus ($E$) | 71.7, MPa |
| Poisson's Ratio ($\nu$) | 0.33 |
| Steel Sleeve | |
| Elastic Modulus ($E$) | 210.0, MPa |
| Poisson's Ratio ($\nu$) | 0.30 |

## 5.4 Mesh Design

The elastic and elasto-plastic materials were meshed in three-dimensions using eight-node linear brick elements. It has been suggested in the literature, [Ismonov, 2009a], that using linear elements perform better than quadratic elements when modeling plasticity. The rigid components were created as a shell, formed from four-node three-dimensional bilinear rigid quadrilateral elements. The mesh on the plate was designed so there would be higher resolution in the vicinity of the hole, where stress and strain change rapidly. This was accomplished by partitioning the plate into an inner and outer region, seen in Figure 5.1 and Figure 5.6. The inner region has a diameter equal to three times the diameter of the hole and is centered about the hole. It is necessary to reduce the mesh density away from the hole in order to reduce the total number of elements in the model and allow for faster run times.

Different mesh configurations were examined to determine what was required to simulate expansion. Early meshes were found to be too coarse and did not have the necessary resolution to capture the plastic deformation occurring near the hole. This was particularly true near the entrance and exit surfaces of the plate where there was a rapid change in the amount of plastic deformation. Without calculating the yielded areas properly, the residual stress fields did not produce accurate results. For this reason, a non-uniform mesh distribution was used, with smaller elements near the entrance and exit surfaces and along the bore of the hole. The mesh density for each model is described by the number of elements through the thickness and the number of radial elements in the inner region. In many cases, a bias is used to increase the density of elements in a particular area. In the radial direction, a single bias was used making the elements at the outer radius of the inner region a number of times larger than the elements near the edge of the hole. In a similar way, a double bias was used through the thickness to increase mesh density at the free surfaces, with elements at the mid-thickness being a number of times larger than the elements at the edges.

The plate mesh is shown in detail using Figure 5.9. The mesh chosen for the “baseline” model has an inner region consisting of 30 elements through the thickness and 30 radial elements. A double bias is used in the through thickness direction so those elements near the entrance and exit surfaces are $\frac{1}{15}$ the size of the elements at the mid-thickness. In the radial direction the elements are biased so that those near the bore of the hole are $\frac{1}{15}$ the size of the elements at the edge of the inner region. This mesh was chosen due to its low number of

elements and its ability to capture the residual stress effects seen in higher mesh models. The low number of elements meant that it was possible to run models on personal machines and did not require the use of a super computer.

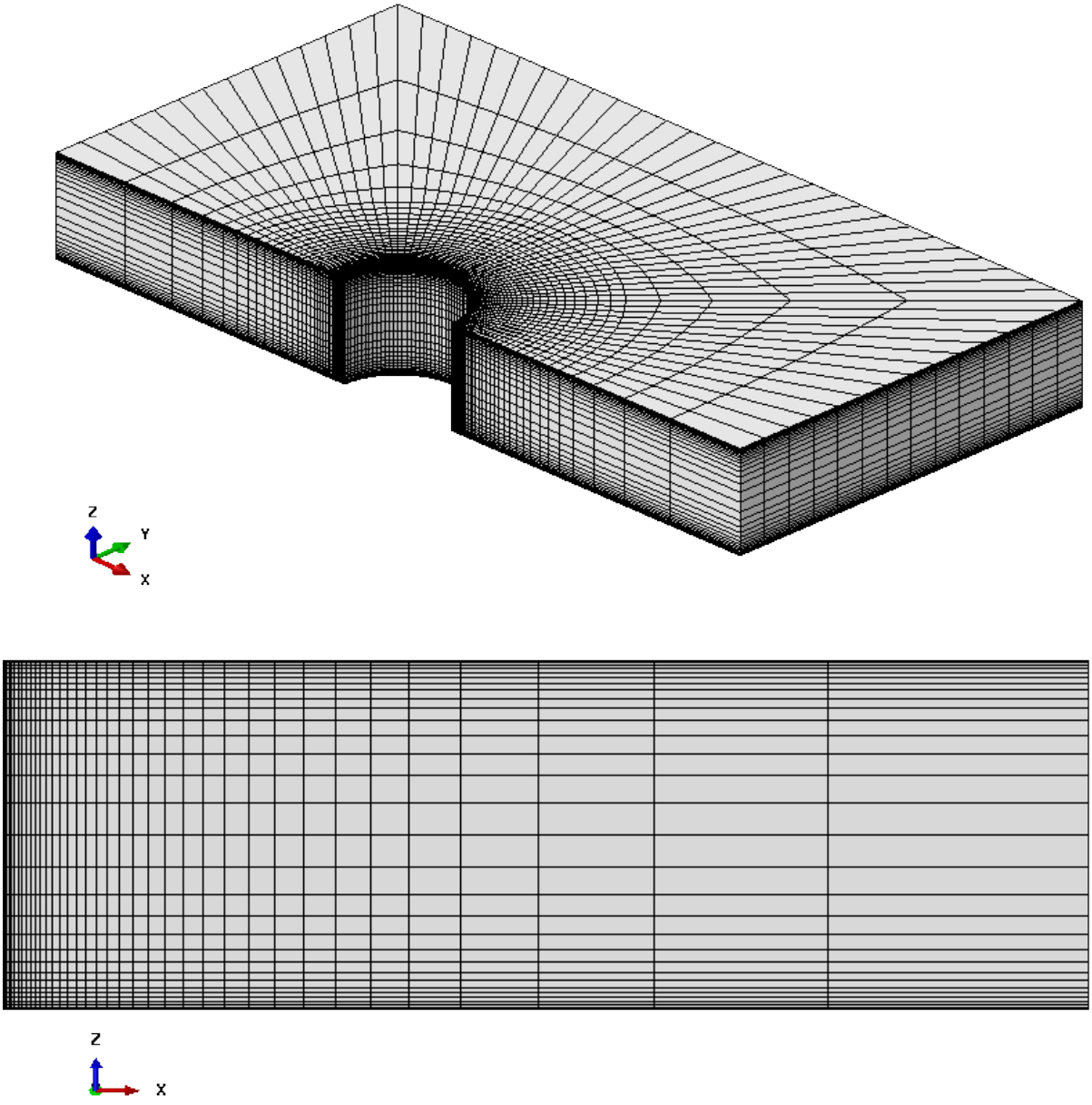


Figure 5.9: Isometric view of the plate mesh (top) and close up of the through thickness mesh seen in the *x*-z plane (bottom).

## 5.5 Contact Selection

Interaction between model components was handled using the general contact option in Abaqus. This allows any surface to interact with one another including themselves. The contact

itself was defined using frictionless tangential properties and “hard” contact to control normal interactions. Nominally, “hard” contact prevents the penetration of one surface through another, but it was necessary to modify this condition using a penalty approach that allowed some penetration to occur. This was necessary to obtain model convergence.

## 5.6 Model Alterations

Variations of the “baseline” model were created for comparison to analyze the effect of specific geometries on the residual stress field. Models with different sized holes were created by making small changes in the script used to generate the model. Multi-plate models where created by generating two-plates and appropriately positioning them in the assembly. Extended models were created by attaching beam elements to the ends of the plates and applying the fully fixed boundary condition to the opposite ends of the beam. In this way it was possible to simulate a clamping condition farther from the expansion hole without adding a large number of elements. A counter-sink was used with the extended model to prevent excessive displacement in the *z*-direction. The design for the counter-sink hole is shown in Figure 5.10. In this model, the edge of the hole at the exit surface has been modified and a nosecap has been added. The addition of the counter-sink to the plate geometry required a reworking of the mesh, which was done in such a way to make the model as comparable as possible to the “baseline”. The FTI guidelines recommend using a straight sleeve along with a nosecap to apply the expansion to the counter-sink surface. Model dimensions for the nosecap were not known, so proportions were chosen such that it could serve its purpose for a given hole size.

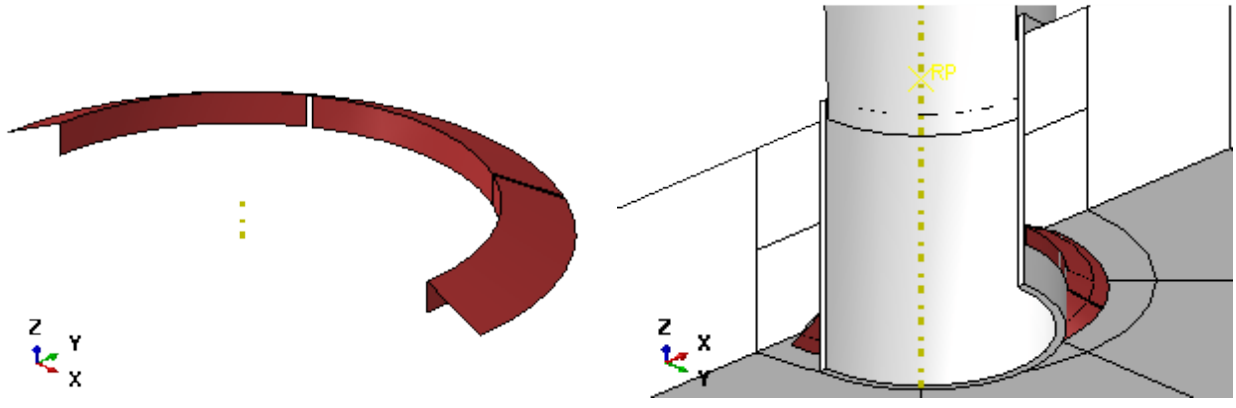


Figure 5.10: Modeled portion of the nosecap (left) and counter-sink assembly (right).

The “baseline” model and variations were all generated using the same Python script. This script allows for interactive assignment of geometric values, like those seen in Table 5.1, and the inclusion of model options. Model parameters that can be generated include multiple plates, friction, split sleeve, flared sleeve, counter-sink hole, and plate extension.

# 6 Results

A number of modified models were created and successfully run to determine how specific variations can affect the residual stress field. Modifications to the “baseline” model include variations in the hole diameter, inclusion of various two-plate configurations, the addition of a counter-sink, and plate extensions to move the boundary conditions. For comparison purposes only two materials are considered, Al 7075 and Al 2024. All plates made of Al 7075 will have the dimensions specified by the “baseline” model and a thickness of 6.88 mm, while the “baseline” for Al 2024 plates will have the same measurements in the *x-y* plane, but a thickness of 6.6 mm. Figure 6.1 gives a short hand notation for the plates associated with each model configuration that will be analyzed.

Table 6.1: Shorthand notation for the model configurations

| Model Description | Shorthand |
|---|---|
| "Baseline" Model | |
| Al 7075 | #1.1 |
| Al 2024 | #1.2 |
| Hole Variations for Al 7075 | |
| $\Delta = (D_{max} - D_{min})/2$ | |
| $D = D_{min} + \Delta = 6.007$ mm | #1.1.1 |
| $D = D_{min} + 2\Delta = 6.045$ mm | #1.1.2 |
| $D = D_{min} + 3\Delta = 6.083$ mm | #1.1.3 |
| $D = D_{min} + 4\Delta = 6.121$ mm | #1.1.4 |
| $D = D_{min} + 5\Delta = 6.159$ mm | #1.1.5 |
| $D = D_{min} + 6\Delta = 6.187$ mm | #1.1.6 |
| Two-plate stack, 0.075 mm spacing | |
| Al 7075 | #2.1 |
| Al 2024 | #2.2 |
| Two-plate stack, 0.100 mm spacing | |
| Al 7075 | #3.1 |
| Al 2024 | #3.2 |
| Two-plate stack, 0.125 mm spacing | |
| Al 7075 | #4.1 |
| Al 2024 | #4.2 |
| Two-plate stack with extensions and counter-sink Al 2024 plate, 0.1 mm spacing | |
| Al 7075 | #5.1 |
| Al 2024 | #5.2 |

## 6.1 Interpretation of the "Baseline" Model

To understand why the residual stress fields are different between configurations, it is first necessary to understand the residual stress field in the "baseline". This requires examining the factors that lead to residual stress formation.

### 6.1.1 Residual Stress Fields

It is important to remember that the process of cold expansion is highly three dimensional and leads to a complex residual stress field, seen in Figure 6.1. All measurements taken for analysis use a cylindrical coordinate system, $S11 = \sigma_{rr}$, $S22 = \sigma_{\theta\theta}$, and $S33 = \sigma_{zz}$. Remembering that the mandrel starts above the plate and moves in the –*z* direction, the top of the plate will be the entrance surface and the bottom will be the exit. It should be noted that there are significant residual stresses in all principal directions with the greatest maximum and minimum both occurring in $\sigma_{\theta\theta}$. All results considered are taken from the cross-section of the plate that exists in the positive *x*, positive *z* plane, illustrated in Figure 5.4 as surface (A).

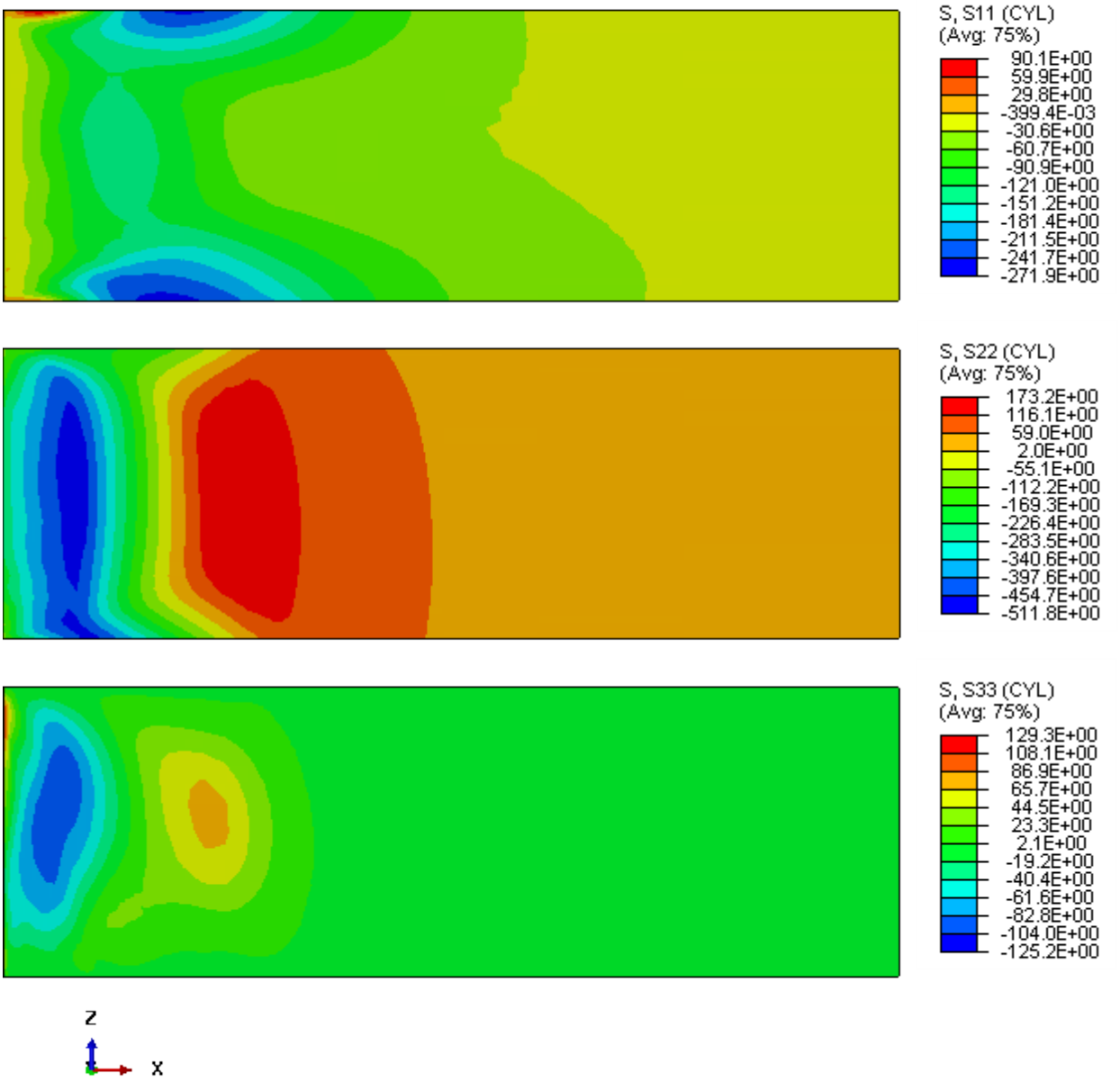


Figure 6.1: The residual stress fields for the "baseline" case displaying the stress in each of the principal directions. Note that the stress levels differ between contours as indicated by the legends on the right and all values are in MPa.

A number of points can be made by simple inspection of the predicted residual stress field. While the top and bottom of the plate both exist as free surfaces, the motion of the mandrel yields slightly different residual stresses in these locations. The free surfaces differ greatly from the mid-surface, with the middle 50% of the plate showing fairly constant values of stress in all principal directions. Compressive residual stress effects extend away from the hole farther at the free surfaces than at the mid-thickness.

### 6.1.2 Plastic Strain Fields

All aspects of the residual stress field are the result of the plastic strain zone generated during the expansion process and the elastic recovery that follows. An interesting point of note is the hourglass shape seen for the residual stress field in both the radial and tangential stress directions. This phenomenon is a direct result of the variations in the plastic zone through the thickness of the plate, Figure 6.2.

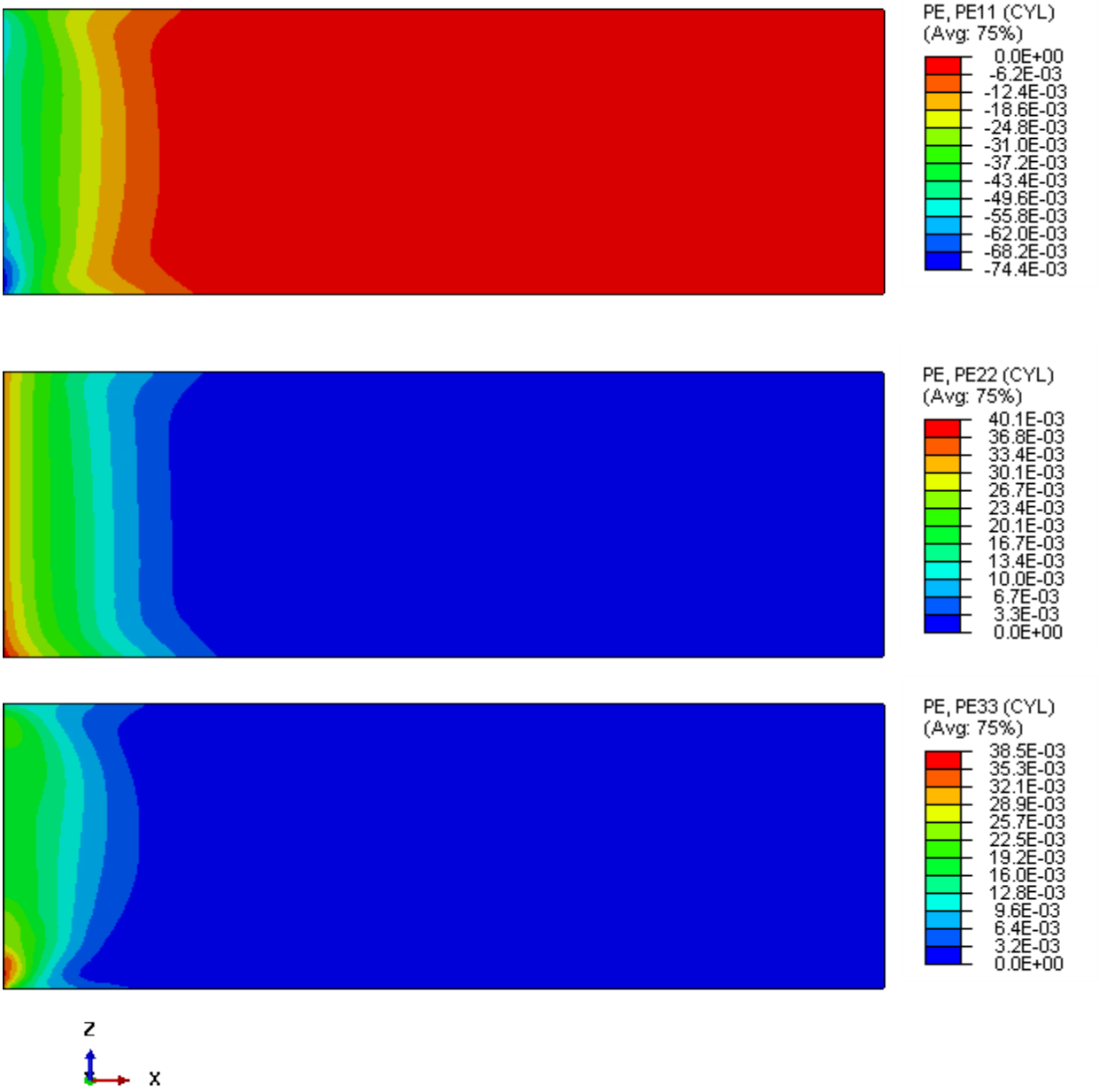


Figure 6.2: The plastic strain fields for the “baseline” case displaying the strain in each of the principal directions. Note that the strain levels differ between contours as indicated by the legends on the right.

### 6.1.3 The Hydrostatic Effect

The smaller size of the plastic zone in the mid-thickness is due to hydrostatic effects caused by the surrounding material. While radial and tangential stresses experienced during expansion may be similar through the thickness of the model, the addition of the axial stress, $\sigma_{zz}$, seen in the mid-thickness causes a net reduction in the deviatoric stress. This creates a

strengthening effect and reduces the radius of the plastic zone. A comparison of the hydrostatic stresses seen during expansion near the free surfaces and mid-thickness are shown in Figure 6.3. Note that the hydrostatic stress seen as the mandrel passes through the mid-thickness (frame 48) is much higher than that experienced during the entrance or exit.

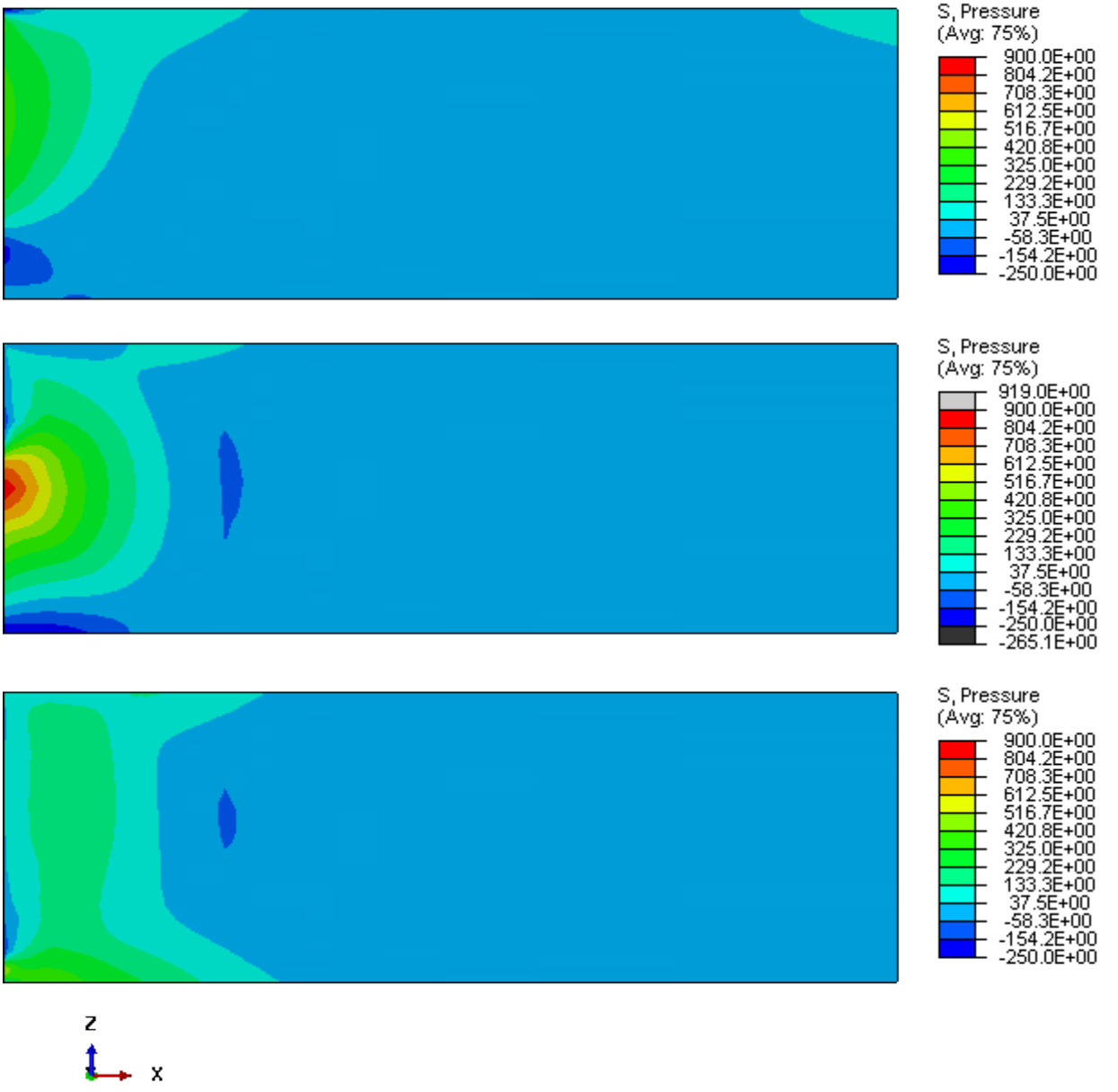


Figure 6.3: Comparison of the hydrostatic stress (pressure) seen at different frames during the expansion process, frame 14 (top), frame 48 (middle), and frame 60 (bottom)

### 6.1.4 Interesting Points

Plastic strain directly affects the residual stress field by creating the shape upon which elastic recovery will occur. It is important to notice that the limit of the plastic zone in the tangential direction corresponds to the maximum stress in this direction, shown in Figure 6.4. This phenomenon has been shown in simpler cases and can be explained using a superposition of loads. One such case is that of a bending beam, where an expanding plastic zone can be seen when moments are applied to the beam ends. Figure 6.5 illustrate the bending of a beam using a sufficiently large moment to cause yielding, followed by the removal of the load to allow relaxation of the beam. Figure 6.6 gives a visual representation of the beam's internal loads and restoring forces. The use of the superposition method adds these loads together to characterize the load necessary to produce the residual stress field seen in the beam. It can be seen that this idea leads to a maximum stress at the edge of the plastic zone. This is due to the plateauing of the internal load as the plastic deformation occurs, coupled with the elastic load that continues to increase with strain. Parallels can be drawn to the case of the expanding hole by conceptualizing the internal loads and elastic forces arising during the expansion process. The deformation caused as the mandrel passes through creates internal loads, while the deformed material, and the undeformed material beyond it, exhibit elastic forces to restore their initial position. The use of superposition, again, leads to a situation where a local stress maximum is created at the edge of the plastic zone.

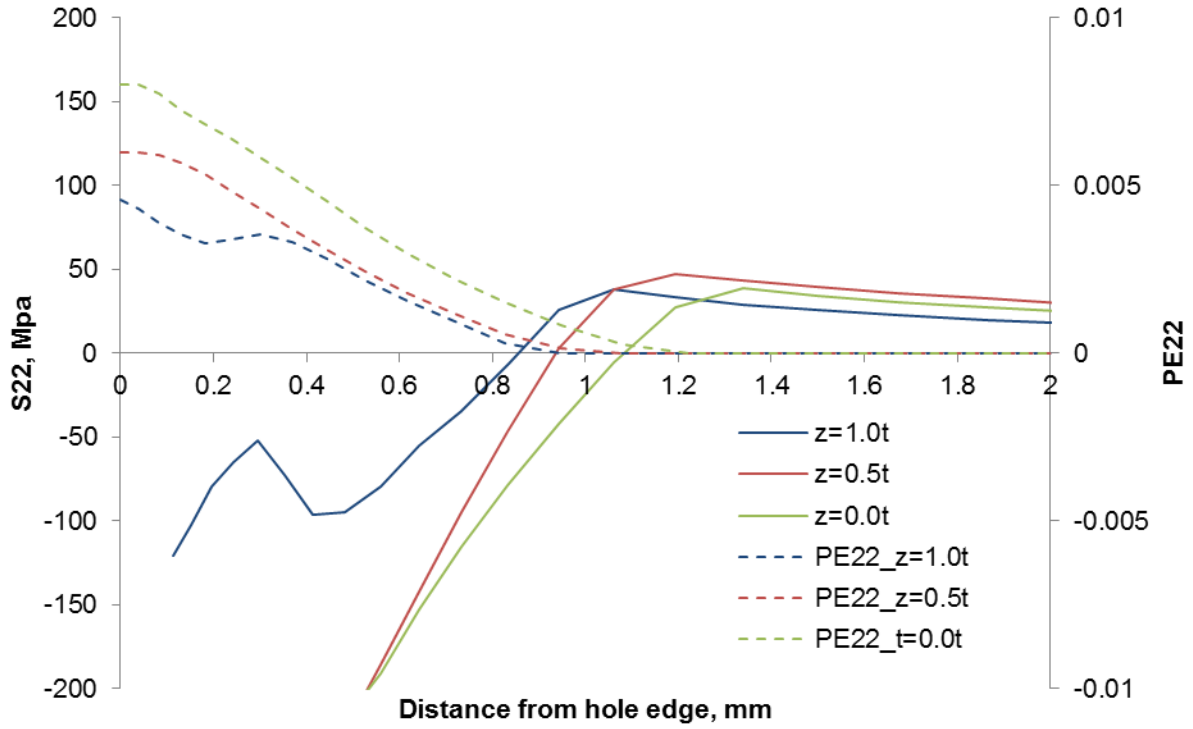


Figure 6.4: Comparison of the tangential stress and plastic strain at different through thickness values.

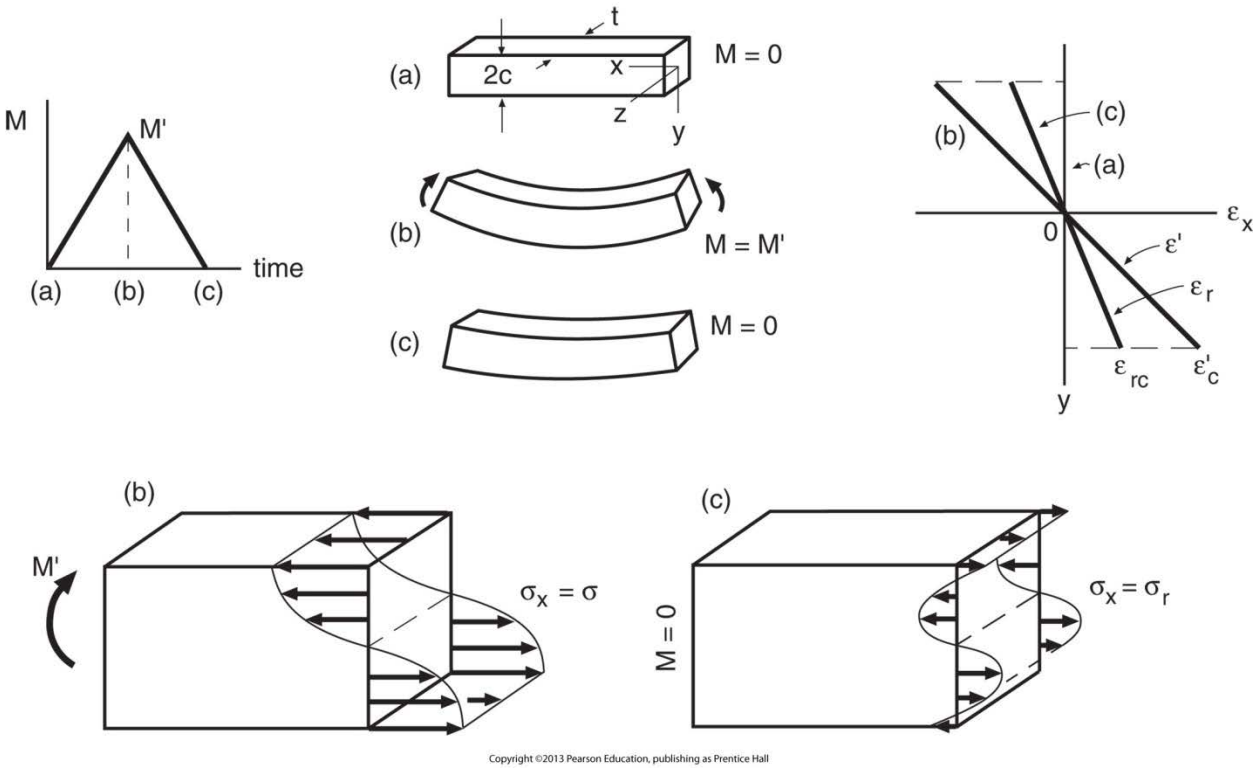


Figure 6.5: Loading of a rectangular beam beyond the point of yielding, followed by unloading. Loading starts from zero moment at time (a) and proceeds to the maximum moment *M*' at time (b). When unloading is complete at time

(c), residual strains $\varepsilon_r$ having a linear distribution remain, and residual stresses $\sigma_r$ are distributed as shown [Dowling, 2013 p.686].

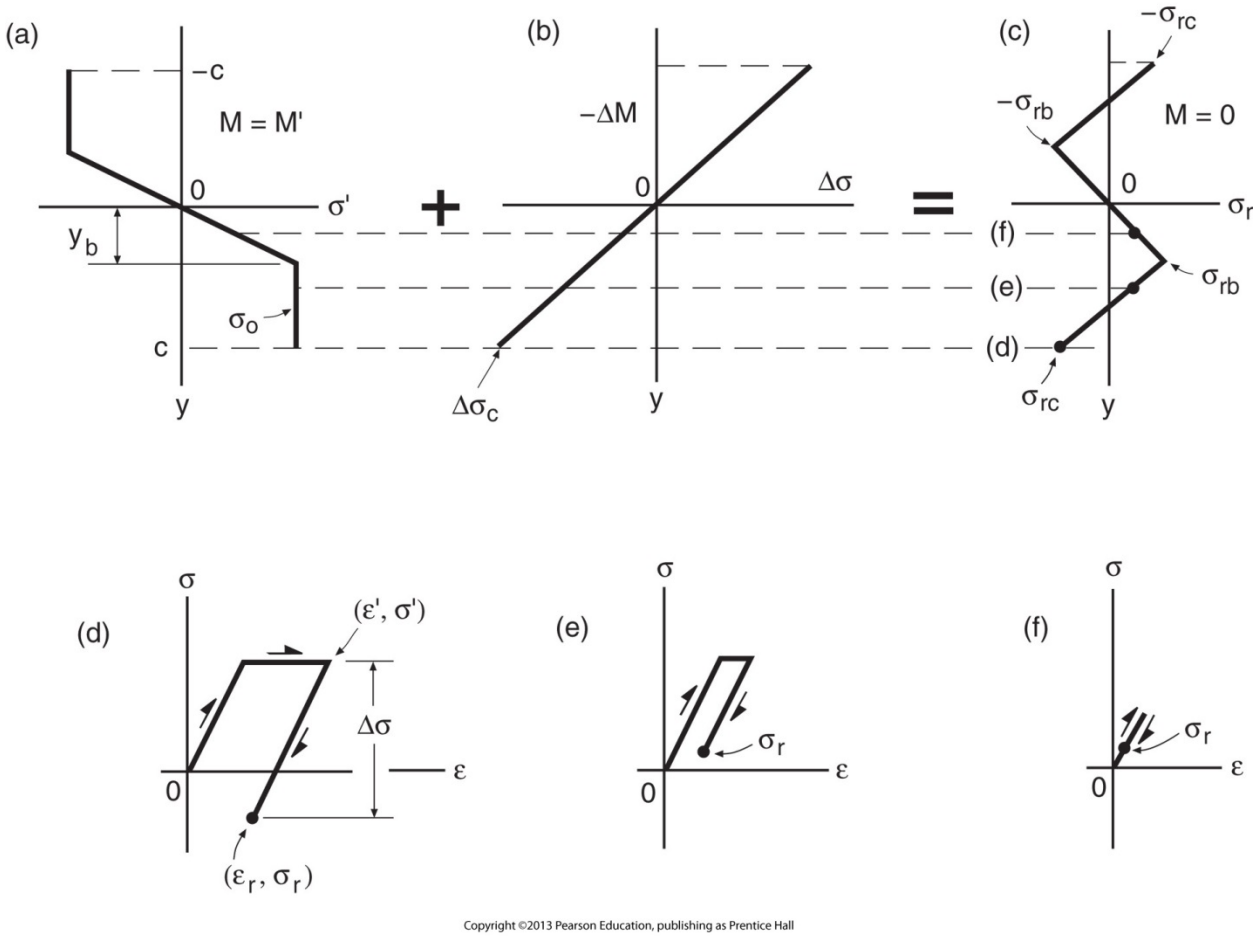


Figure 6.6: For a rectangular beam of an elastic, perfectly plastic material, stresses at the maximum moment are shown in (a), stress changes during unloading in (b), and residual stresses in (c). Depending on the location, residual stresses may be opposite in sign to the maximum stress (d) or of the same sign (*e*, *f* ). The particular case illustrated corresponds to $M' = 0.95M_o$[Dowling, 2013 p.687].

An additional point of interest is that the location of minimum stress in the tangential and radial direction occurs at the farthest extent of reverse yielding. This point can only be illustrated by looking at the time history of plastic strain. Unfortunately, time history of stress and strain cannot be shown be for the nodes of this finite element model. This is due to the way these values are calculated, and can therefore only be displayed properly for integration points attached to elements. Figure 6.7 shows the history of plastic strain in the tangential direction for two adjacent elements that straddle the point of maximum compression near the mid thickness.

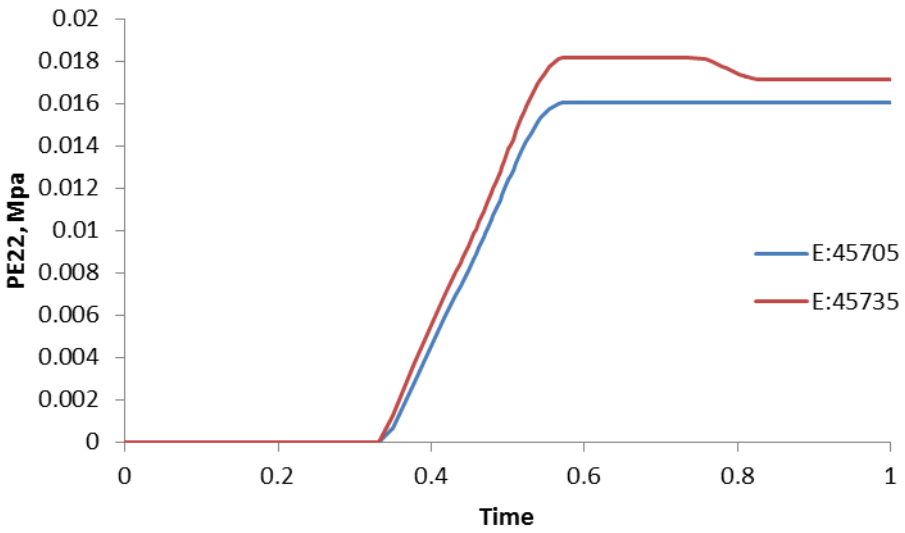


Figure 6.7: Plastic yielding in the tangential direction for elements straddling the point of minimum residual stress

It has been stated many time that the three dimensional state of stress is complex and difficult to duplicate without simulating the full mandrel expansion. This point is supported by the through thickness variations in stress and strain, seen above in Figure 6.1 and Figure 6.2. It can be further demonstrated by examining the plastic shear strain in the *r*-z plane. This strain, shown in Figure 6.8, clearly illustrates significant amounts of deformation occurring in the *r*-z plane, particularly at the exit face for the plate. This effect would not occur if uniform pressure or incremental expansion methods were used to approximate the expansion.


Figure 6.8: The *r*-*z* plastic shear strain fields for the “baseline” case.

## 6.2 The Effect of Hole Size Variation

A comparison of different models with increasing hole size will demonstrate how sensitive the residual stress field can be to changes in the starting hole diameter.

### 6.2.1 Using Line Graph Analysis

The gradient maps presented so far can only give a general understanding of the residual stress field and the plastic strains that created them. It can be difficult to recognize changes in stress using only a gradient map like those above. In order to make useful comparisons, standard line graphs will be used. Unfortunately, a single line graph can only display information along a series of points. In order to give a more complete picture, multiple lines are given at varying locations. By making these comparisons, aspects of the field can become more obvious. Line graphs can make interesting trends in tangential stresses more overt. Figure 6.9 gives the tangential stress for the "baseline" model at different locations through the thickness of the plate.

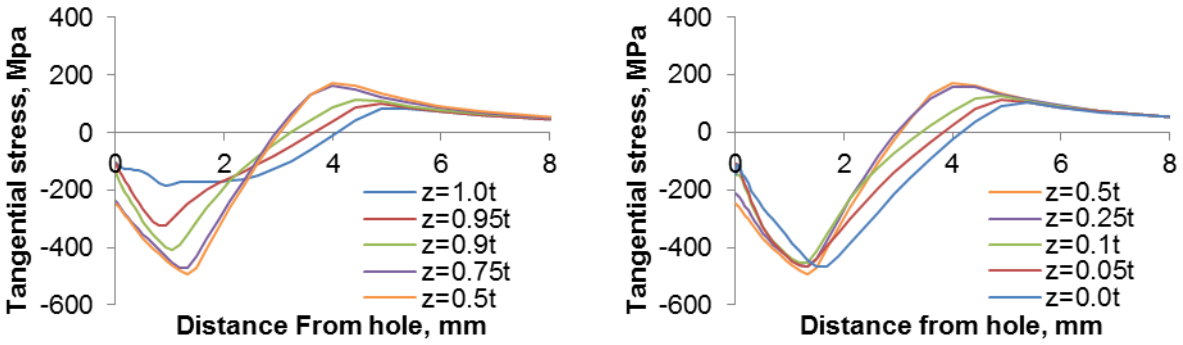


Figure 6.9: Evolution of the tangential stress through the thickness for a plate with hole diameter of 5.969 mm (#1.1), showing the top half of the plate (left) and the bottom half of the plate (right).

It is interesting to note, that starting from the entrance surface and going to the mid surface there is a continuous increase in the magnitude of the compressive stress. Additionally, the point of maximum compressive stress moves farther from the hole edge. However, in the bottom half of the plate the compressive stress remains constant at the yield stress for the material and there is very little variation in its location until the exit surface of the plate. As a tool to combat fatigue cracking, these graphs explain why it is more common to find propagating crack at the entrance surface when compared to the exit.

Beginning with hole size variation, these types of line graphs will be used to carry out a majority of the analysis. Starting from the "baseline" model, which has a radius equal to the minimum radius given in the FTI regulation for a ¼ in hole expansion, the hole size was incrementally increased while maintaining the same dimension on the mandrel.

### 6.2.2 Variation of Starting Hole Size

The purpose of this series of models is to determine how the residual stress field is affected if starting holes are accidently oversized. The increment used to increase the hole size is equal to half the difference between the allowable hole sizes, $\Delta = (D_{max} - D_{min})/2$ . The hole size was incremented six times, creating models where the hole diameter is larger than the maximum recommended starting size. This was done as a point of interest to determine the point at which the hole diameter begins to detrimentally affect the residual stress field. If the hole was made smaller than the recommended size it would most likely cause additional damage to the hole surface. This damage would not be shown in the model and it would be difficult to quantify its detrimental effect. The considered hole sizes are given in Table 6.2 along with the shorthand notation associated with each model.

Table 6.2: Shorthand notation for hole variation models

| Model Description | Shorthand |
|---|---|
| "Baseline" Model $D = 5.969$ Al 7075 | #1.1 |
| Hole Variations for Al 7075 $\Delta = (D_{max} - D_{min})/2$ | |
| $D = D_{min} + \Delta = 6.007$ mm | #1.1.1 |
| $D = D_{min} + 2\Delta = 6.045$ mm | #1.1.2 |
| $D = D_{min} + 3\Delta = 6.083$ mm | #1.1.3 |
| $D = D_{min} + 4\Delta = 6.121$ mm | #1.1.4 |
| $D = D_{min} + 5\Delta = 6.159$ mm | #1.1.5 |
| $D = D_{min} + 6\Delta = 6.187$ mm | #1.1.6 |

### 6.2.3 Evolution of Residual Stress Fields Due to Hole Variation

By increasing the hole diameter, the interference between the mandrel and plate is lessened. In general, this leads to a plastic zone with a smaller radius, Figure 6.10. A smaller plastic zone will decrease the size of the compressive region. For the mid-thickness, the lack of interference causes the peak compressive stress to occur closer to the edge of the hole due to a smaller reverse yielding zone. It also plays a minor role in the value of the maximum compressive stress, Figure 6.11. As the hole size was increased, the magnitude of the of the compressive load at the mid thickness was increased slightly. From these graphs, it can be seen that the maximum value for the compressive stress is based more on the yield strength of the material than the extent of cold expansion. At the entrance surface of the plate, smaller amounts of interference lead to a smaller compressive residual stress field in both magnitude and area below the x-axis, Figure 6.12. As the hole size approaches the maximum considered, there is a drop off in the magnitude of the compressive stress at all points through the thickness. If hole size is increased further, this weakening of the residual stress field will continue until no plastic deformation occurs and the residual stress field is non-existent. This drop off in the maxima is more difficult to see at the surface due to a more complicated stress profile, but can still be observed at the point of maximum tension. One noticeable effect as this drop off begins is the reduction in peak compressive stress at the exit surface of the plate. This is shown in Figure 6.13 when looking at the evolution of stress through the thickness of plate.

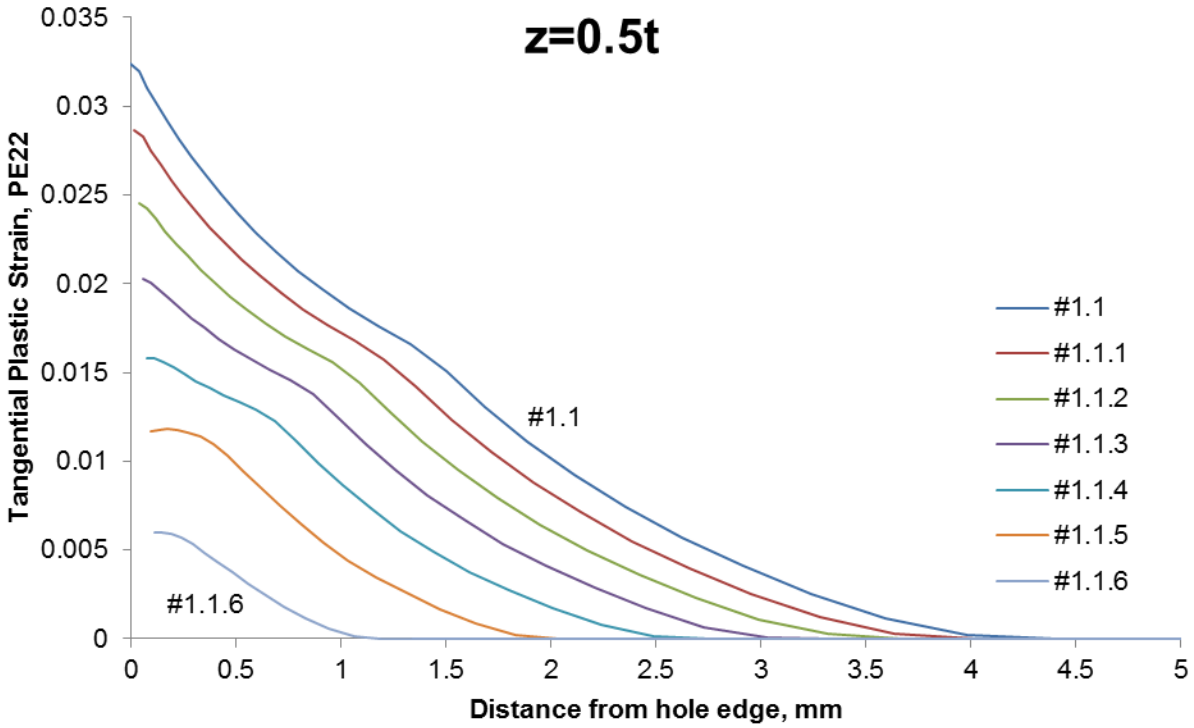


Figure 6.10: Comparison of plastic zone at the mid thickness for plates with hole sizes ranging from $D = 5.969$ to 6.187mm

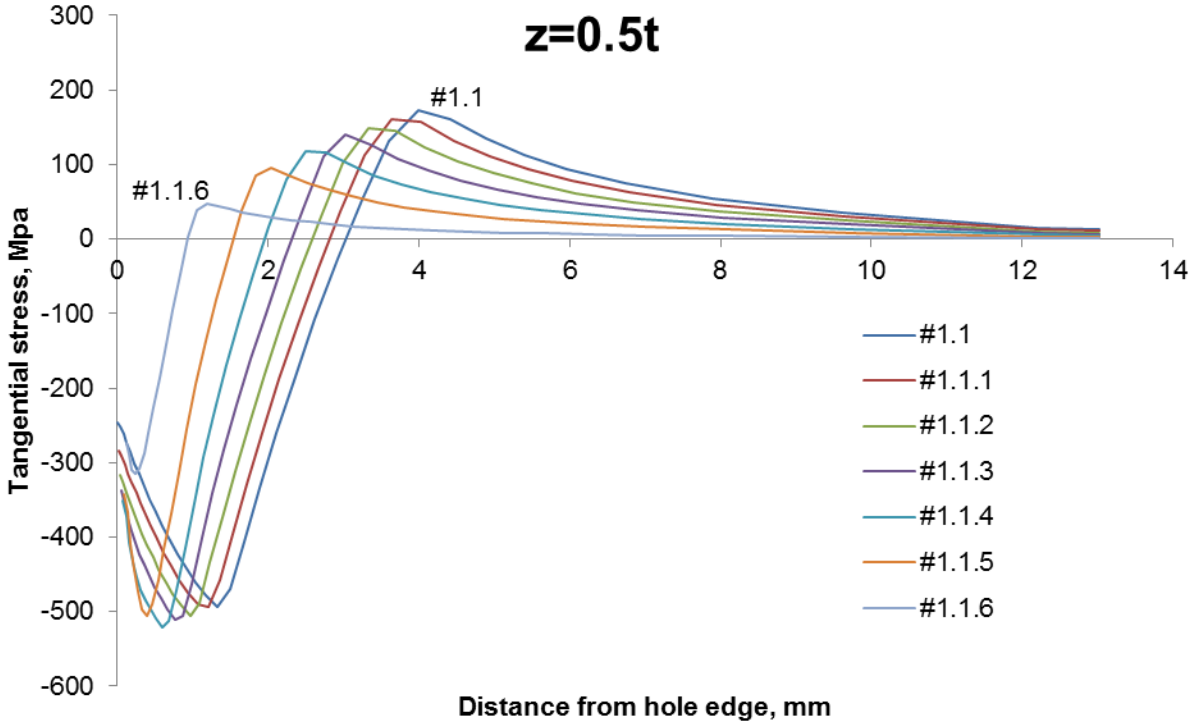


Figure 6.11: Tangential stress at the mid-surface for plates with starting hole sizes ranging from $D = 5.969$ to 6.187 mm.

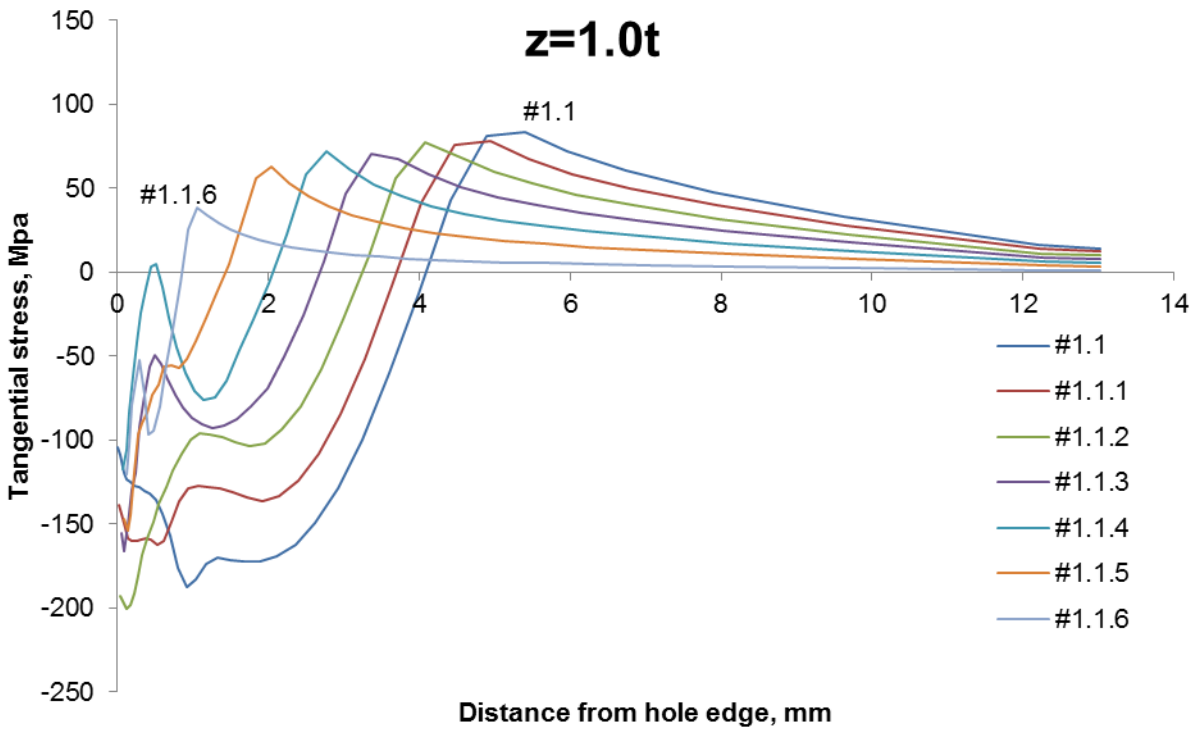


Figure 6.12: Tangential stress at the top surface for plates with starting hole sizes ranging from $D = 5.969$ to 6.187 mm.

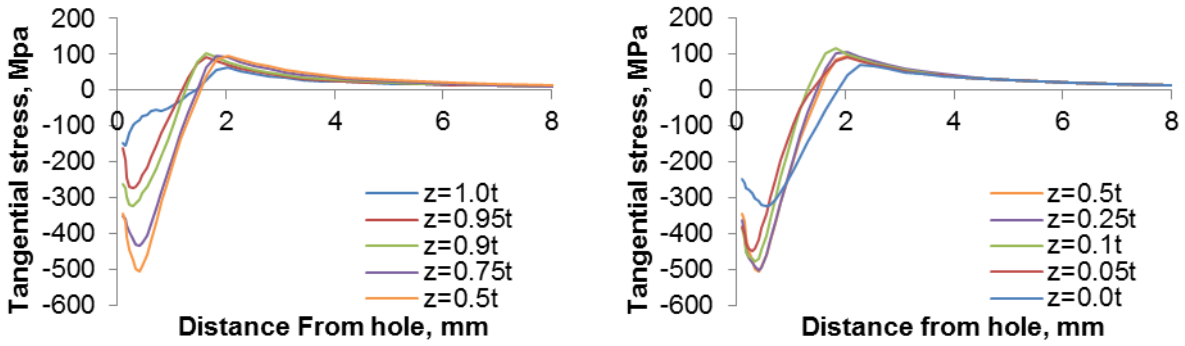


Figure 6.13: Evolution of the tangential stress through the thickness for a plate with hole diameter of 6.159 mm (#1.1.5), showing the top half of the plate (left) and the bottom half of the plate (right).

## 6.3 The Effect of Simultaneous Two-Plate Expansion

The level of interference between components during the expansion process is crucial to how the plastic zone and by extension the residual stress field forms. With the addition of a second plate, interference is created between previously free surfaces. This leads to a partially constrained situation between adjacent plates. The effect of the constraint can be considered

similar to the hydrostatic stress effects seen at the mid surface of the plate. This constraint acts to increase the strength of the material in the region near the contact of both plates.

### 6.3.1 Two-Plate parameters

The addition of the two-plate effect to the problem also adds another variable, the distance of separation. For this work, the separation distance was varied between three models. A final model was also created in which the boundary conditions were moved away from the hole to simulate clamping at a greater distance. The extended two-plate model also included a counter-sink and nosecap on the bottom plate. The shorthand notation for all plates used for two-plate simultaneous expansions are given in Table 6.3.

Table 6.3: Shorthand notation for the model configurations using two-plates

| Model Description | Shorthand |
|---|---|
| “Baseline” Model | |
| Al 7075 | #1.1 |
| Al 2024 | #1.2 |
| Two-plate stack, 0.075 mm spacing | |
| Al 7075 | #2.1 |
| Al 2024 | #2.2 |
| Two-plate stack, 0.100 mm spacing | |
| Al 7075 | #3.1 |
| Al 2024 | #3.2 |
| Two-plate stack, 0.125 mm spacing | |
| Al 7075 | #4.1 |
| Al 2024 | #4.2 |
| Two-plate stack with extensions and counter-sink Al 2024 plate, 0.1 mm spacing | |
| Al 7075 | #5.1 |
| Al 2024 | #5.2 |

### 6.3.2 Comparison of Maximum Interference

With each of these changes in separation distance, the amount of interference should change. To determine this change in interference between models, the axial (z-direction) stress was examined for each case. In the two-plate models examined here, Table 6.3, two maxima were encountered for the radius of contact. As the maximum diameter of the mandrel approaches the plate interface an interference maxima can be found with a peak in the radius of contact. As the mandrel continues through the two-plate stack-up, the contact radius decreases as the maximum diameter of the mandrel passes through the interference surface. After this, the radius of contact increases to another maximum as the mandrel is pulled through the bottom plate. While the evolution of stress from one maximum to the next is difficult to capture, the comparison of the interface stresses is given in Figure 6.14.

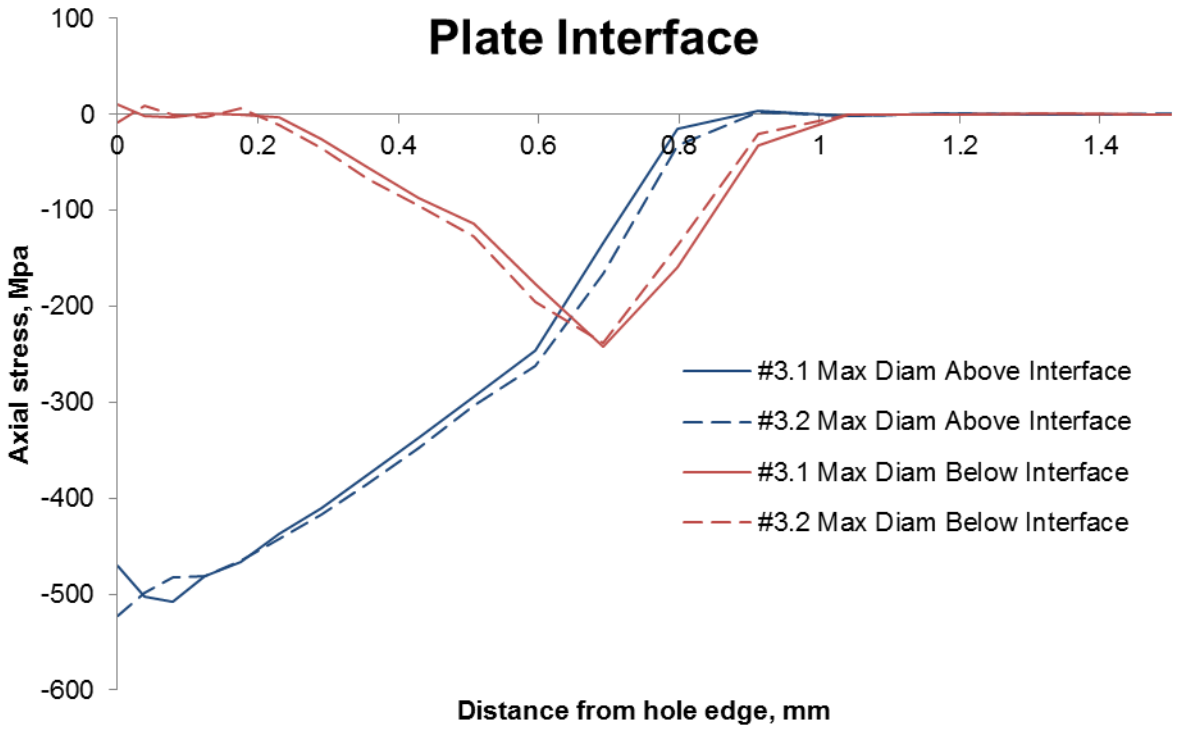


Figure 6.14: Axial stress, $\sigma_z$, at the exit of the top plate (#3.1) and entrance of the bottom plate (#3.2) for the two maxima of contact.

In both cases the axial stress at the exit of the top plate and entrance of the bottom plate match very well, as they should to maintain force equilibrium. It can be seen that when the second maximum radius of contact occurs, the contact is only a ring and does not extend from

the hole edge. The maximum values of stress are also much lower after the maximum diameter of the mandrel has passed through the interface. It is therefore assumed that the first maxima of contact is probably the more crucial for the development of the residual stress field and will be used to make comparisons between models with different spacing, Figure 6.15. As the gap opening is increased, the contact zone between the plates decreases. When the extensions were added, the contact zone also decreased. In addition to a decrease in the contact area when the extensions were used, there was also a decrease in the axial stress as compared to the short models. Looking at the magnitude of the axial stresses, it is interesting to note that the short models share magnitudes fairly close to each other and have trends that look nearly identical. The lower magnitudes for axial stress in the case of the extended model can be due to the ability of both plates to bend in the *z*-direction, lessening the amount of interference.

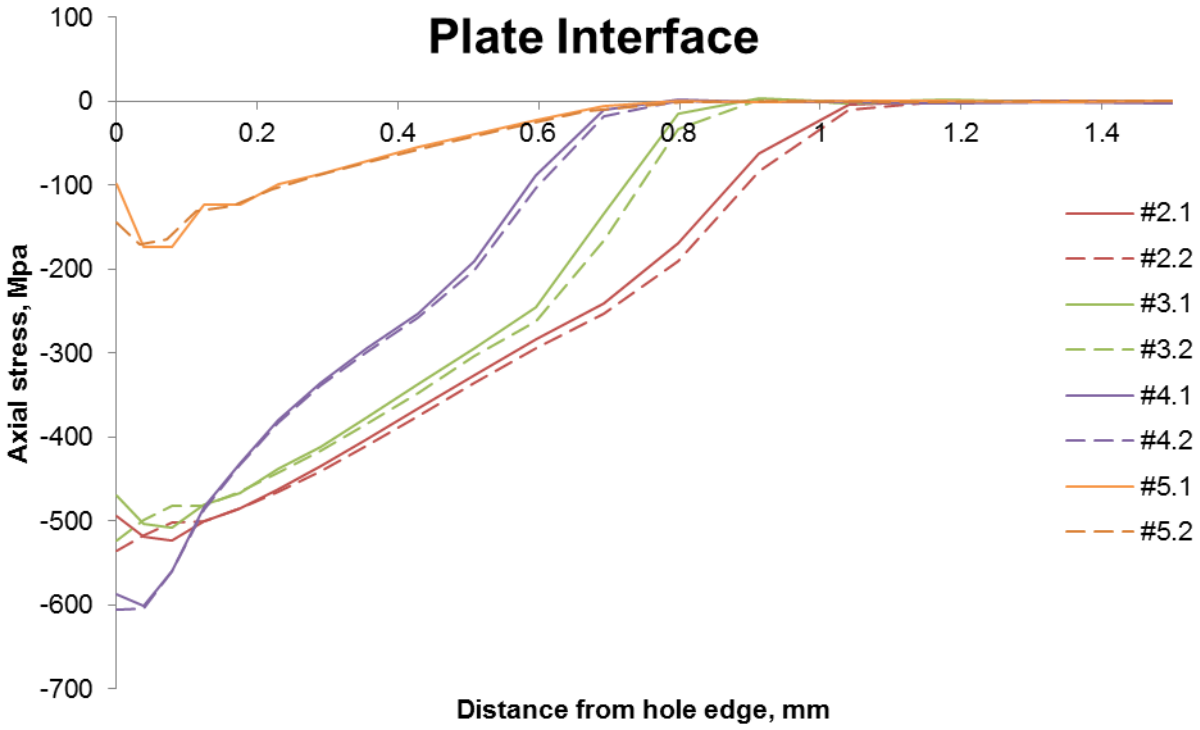


Figure 6.15: Axial stress at the exit of the top plate (.1) and entrance of the bottom plate (.2) during the first period of maximum contact.

### 6.3.3 Comparison of Two-plate Model to the "Baseline"

Any differences in the residual stress field between the single plate and multi-plate cases will be due to the interference of the plates. The addition of the axial stress at the interface during

the expansion process creates a hydrostatic stress on a previously free surface. This hydrostatic stress effects the development of the plastic strain field in a similar way to stresses seen at the plate mid-thickness. For that reason, it is expected that any major differences will occur at the exit of the top plate, Al 7075, and the entrance of the bottom plate, Al 2024. It is simple to observe, through Figure 6.16, that all the models share the same mid-thickness residual stresses. The only exception may be the case where extensions were used and a more significant tensile force is visible in the area away from the hole.

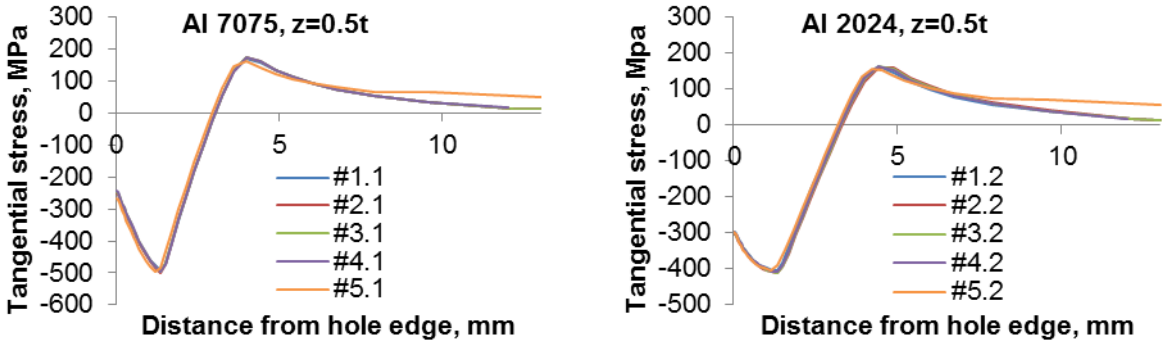


Figure 6.16: Comparison of stress in multi-plate models at the mid thickness for Al 7075 plates (left) and Al 2024 plates (right).

If the mid thickness is fairly unaffected by the two-plate configuration, then it is important to determine how much of the thickness is changed. The most likely location for differences would obviously be where the interference occurred, the exit of the top plate and the entrance of the bottom plate. Figure 6.17 gives a side by side comparison of the lower half of the Al 7075 plate. Figure 6.18 allows a similar comparison for the Al 2024 plate.

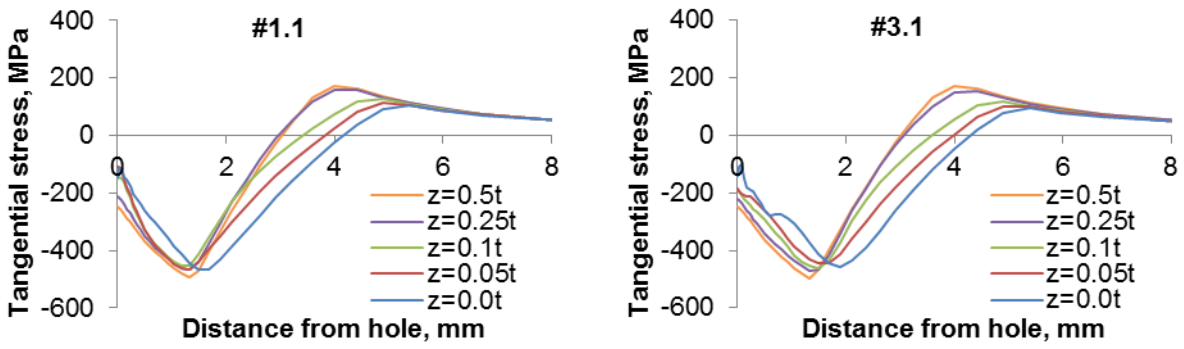


Figure 6.17: Comparison of the residual stress fields for the lower half of Al 7075 that are part of a single plate expansion (left) and the top of a two-plate expansion with 0.1 mm spacing (right).

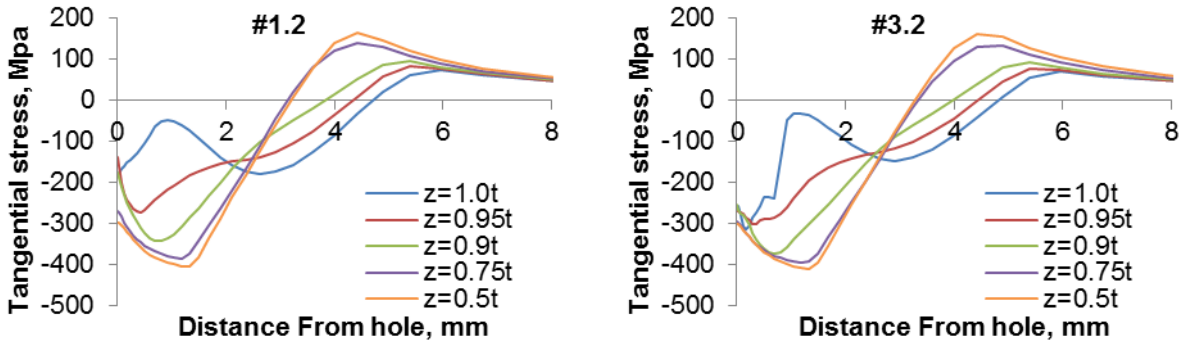


Figure 6.18: Comparison of the residual stress fields for the upper half of Al 2024 that are part of a single plate expansion (left) and the bottom of a two-plate expansion (right).

In the case of the Al 7075 plate there seems to be only a small effect on the residual stresses. Surprisingly, it appears that when the Al 7075 plate is used as the entry plate in a two-plate configuration, the residual stresses in the lower half actually become slightly less compressive. It is evident that in the two-plate configuration the residual stresses continuously decrease while moving away from the mid thickness. This is different from the single plate model where the residual stress field is almost constant up to the free surface.

Analysis of the Al 2024 shows significantly different results when used as the bottom plate in a stack-up. While the mid-thickness values appear very close, stresses near the surface and particularly at the surface become drastically different. It is clearly evident that within the first millimeter of the surface, encompassing about 15% of the thickness, the residual stresses show increased compressive values. This effect is most noticeable along the bore of the hole and near the plate surface. There is clear evidence that in the proximity of the two-plate interference the residual stresses were greatly benefitted.

It is important to note that there is still contact between the plates at the end of the simulation run. At its maximum this contact has an axial stress of 135MPa between the two-plates. This is important because the stress field shown here may differ slightly from the free plate residual stress field.

### 6.3.4 Evolution of Residual Stress Fields Between Two-plate Models

Now that the effects of two-plate interference have been established, it is crucial to understand how changing the spacing between plates affects the results. Figure 6.19 and Figure 6.20 compare results for the Al 7075 and Al 2024 at their respective interface surfaces. Comparison of the exit surfaces of the Al 7075 plate, Figure 6.19, show very consistent results, which support the idea that the top plate is only slightly affected in a two-plate configuration. Close scrutiny of the top plate analysis shows that the configurations with a smaller gap may have some benefit over configurations with larger gaps. All configurations have slightly less compressive values than the single Al 7075 plate.

As previously stated, the entrance surface of the bottom plate is where most of the benefit from a two-plate configuration exists. By comparing the results due to different spacing it can be seen that smaller spacing leads to a more compressive residual stress field near the hole edge. This compressive field is higher in magnitude and extends farther from the hole when the spacing between plates is smaller. While the extended configuration does not achieve the same magnitudes of compressive stress as the shortened two-plate configurations do, its stress stays in a highly compressed state for greater duration away from the hole.

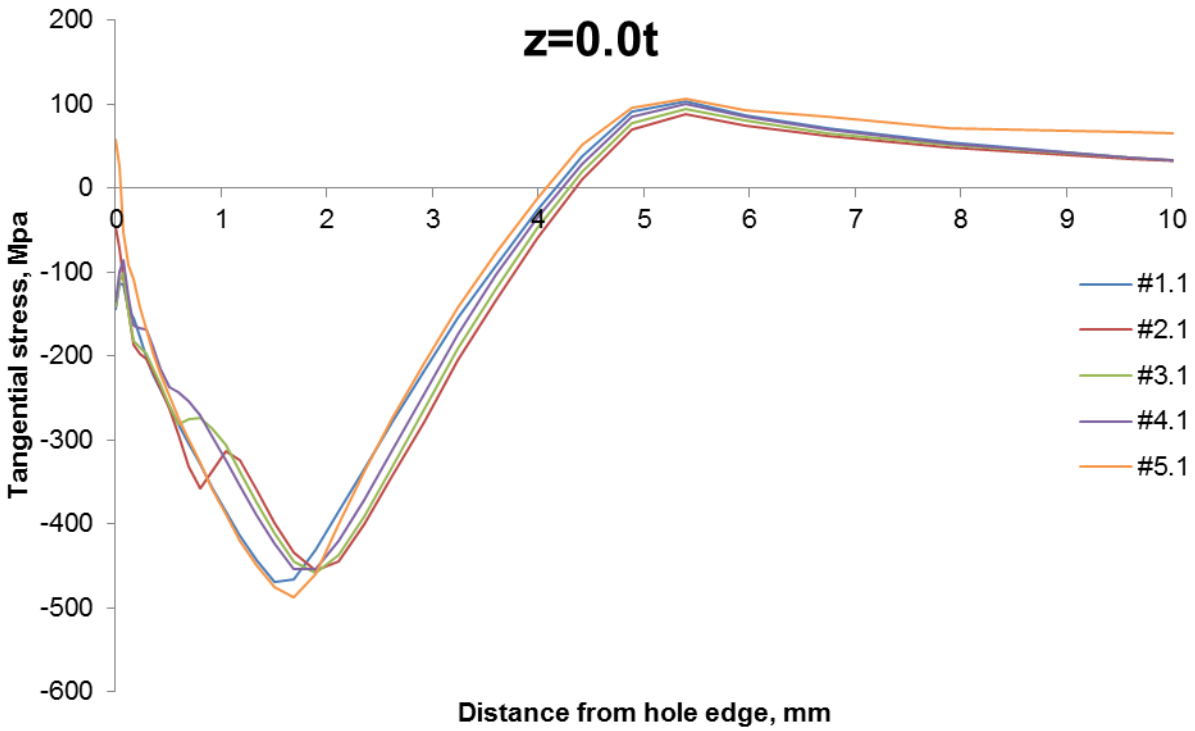


Figure 6.19: Comparison of stress in the two-plate models at the exit surface for Al 7075 plates.

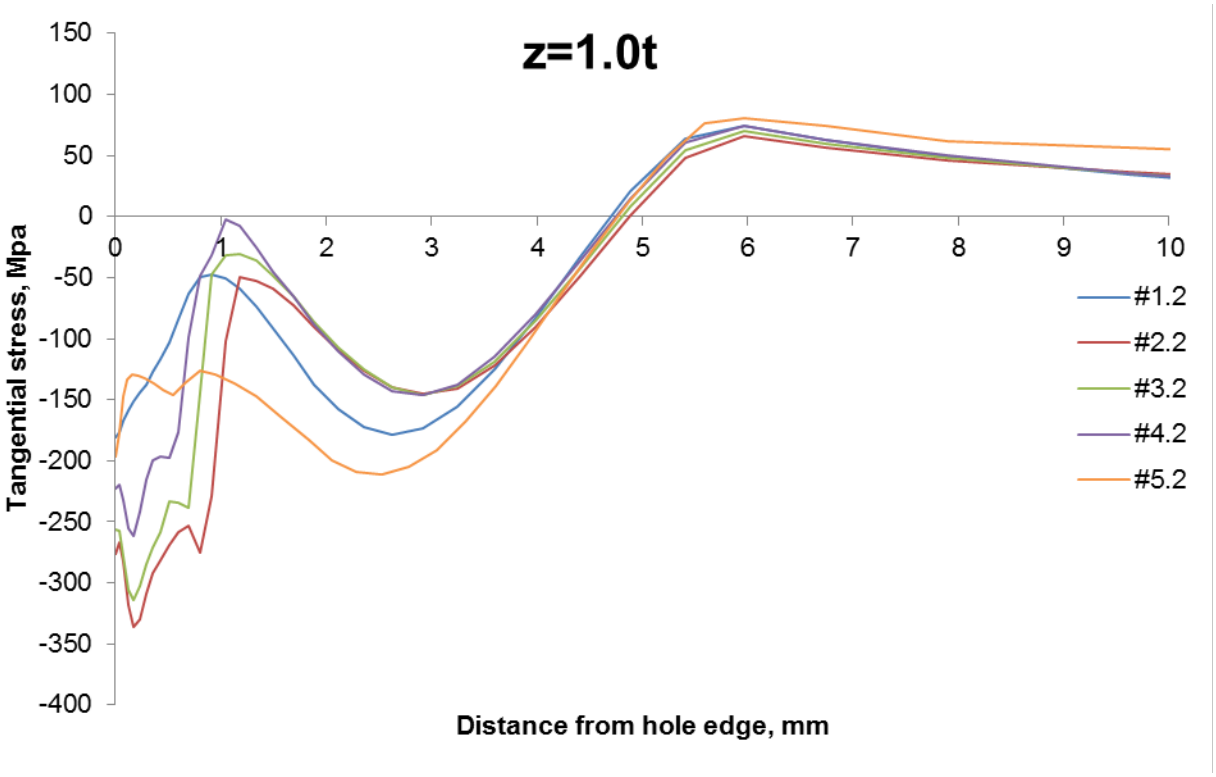


Figure 6.20: Comparison of stress in the two-plate models at the entrance surface for Al 2024 plates.

# 7 Discussion

Throughout this project a number of ideas have been studied through the scripting, modeling, and analysis of results. With the results in mind, it is important to consider that the complicated nature of the model setup and implementation make the introduction of errors possible. Sources of error were reduced, once identified, through iterative generations of the script used to generate the model. This required that certain aspects of the model be simplified or removed to achieve convergence or drastically reduce the run time. Using the models that have been completed, analyses have given insight into the interactions that different variations have with the residual stress field. From this a number of lessons have been learned regarding the nature of cold expansion and how model factors can affect the residual stress fields. Some of the unique results presented above suggest possible improvements to the application of cold expansion in the field. The script developed for this project may be used in the future to continue analyzing additional factors and create a more universal model to examine split sleeve cold expansion.

## 7.1 Model Accuracy

To draw conclusions from the results it is required that the model be sufficiently accurate. This accuracy is achieved through verification and validation of the model. By adjusting the mesh on the model and comparing the results it was possible to determine if the results were converging to the same residual stress field. After verifying that the model was converging to a single result, an appropriate mesh was chosen that reasonably captured important aspects of the results. While this work did not have actual samples to compare to, validation was accomplished by ensuring the results are consistent within the existing work of cold expansion research.

### 7.1.1 Verification

Verification is needed to demonstrate that the model parameters used are appropriate for capturing the relevant results. After examining the original mesh, it was found to be too coarse and did not have the necessary resolution to capture the through thickness plastic deformation that was occurring during the expansion process. As a result, the mesh density was modified in the inner region, immediately surrounding the hole. At first, the mesh was increased in an unbiased way with all elements along a particular direction having the same length. When this

proved insufficient, meshing with a small bias was attempted. Figure 7.1 shows the evolution of the stress field, as the element density was increased near the free surfaces and the hole. After creating models with a higher number of elements, it was determined that only the free surfaces benefitted from an increase in mesh density. For this reason and because this project was started with the idea that the model should be capable of running on a personal machine, the number of elements was dropped, but a higher bias was implemented. In this way, the rapidly changing aspects near surfaces of the model were captured using fewer total elements while maintaining the same accuracy seen in the high element number models. This meshing method does create elements with bad aspect ratios near the bore of the hole, at the mid thickness, and at the entrance and exit surfaces away from the bore. The results in these locations are shown to be fairly constant and do not seem to be a problem. The models chosen for comparison in Figure 7.1 are intended to show the starting point of the model, how it evolved as elements and bias were added, and how the results from the chosen mesh configuration, #1.1, compare to higher mesh models. The shorthand for each model along with their element notation is given in Table 7.1. Here, for example, model #0.3 is established to have 20 elements in the thickness direction and 40 elements in the radial direction, within the inner zone. Further, the elements for model #0.3 are biased so that the smallest elements are 1/10 the size of the largest in the thickness direction, and 1/15 for the radial direction. All models presented in Table 7.1 follow the same convention. The number of elements around the circumference was picked to be 56 for all models and does not use a bias.

Table 7.1: Shorthand notation for the mesh configurations using the form (thickness)x(radius)

| Model Description | Shorthand |
|---|---|
| 32x32, no bias | #0.1 |
| 32x32, biased 6x6 | #0.2 |
| 20x40, biased 10x15 | #0.3 |
| 40x80, biased 10x15 | #0.4 |
| 30x30, biased 15x15 | #1.1 |

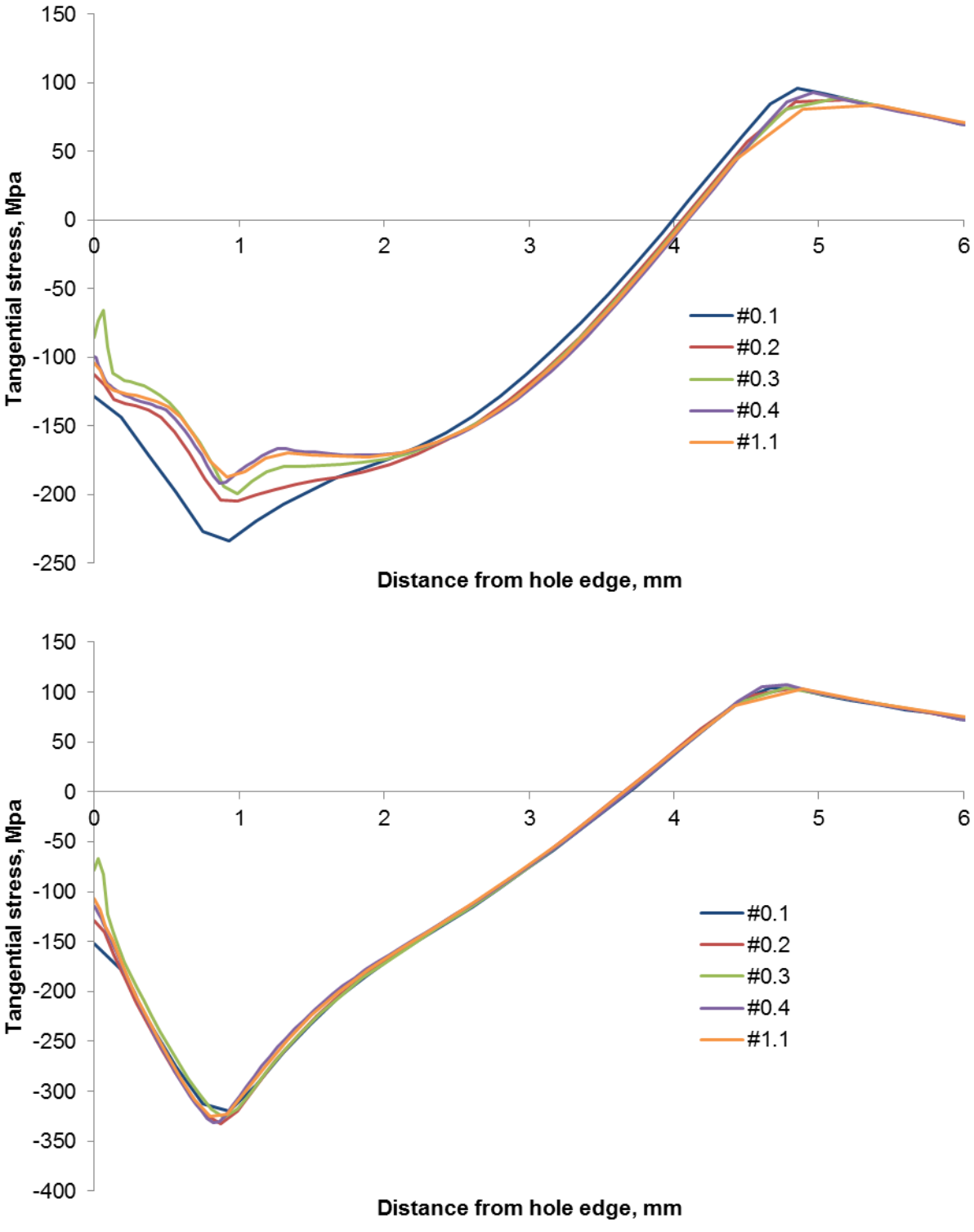


Figure 7.1: Residual stress in the tangential direction at the entrance surface, z=1.0t, (top) and just below the entrance surface, z=0.95t, (bottom).

It is immediately evident that increasing the mesh density serves primarily to improve the results at the entrance surface, while the mid-surface remain consistent across all meshes. The specific minimum and maximum values experienced at the mid thickness are fairly close, except near the bore of the hole , $r = R$, where the values show higher variation. It is clear that most of the improvement was achieved by increasing the density near the free surfaces, which was accomplished most efficiently by using a high bias. The mesh chosen for this work, #1.1, is a biased mesh that used 30 elements through both the thickness and inner radius with a bias of 15 in both zones.

For the situations shown here, changing the mesh on the sleeve did not affect the results and in some cases resulted in the model becoming unstable. It is possible that a higher mesh on the sleeve would have caused some of the unused model variation to run to completion. Unfortunately, due to the limited computer resources this was difficult to analyze as adding an additional row of elements significantly increased the computation time. Another dilemma was that adding elements to the sleeve did not give better resolution in the plate, which is the true target of this analysis.

### 7.1.2 Validation

It was not within the scope of the planned work to run a set of actual tests with which to compare to the data. For that reason, the model will be compared to work previously presented in other academic papers. Due to the flexibility of the model developed here, it is not difficult to recreate the geometries and material properties used in other work as long as the necessary specifications are given. This allows for a side by side comparison of the results given in another work and the results generated using the script developed in this work. To make this comparison possible the original text must include plate dimension, the plate material used, and some reference to the FTI toolkit used to perform the cold expansion. It was important to have either the FTI toolkit number or specific dimension on the mandrel and sleeve to ensure that the degree of cold expansion used was the same as the original paper. This specification was important because, as it has been shown in section 6.2, a small change to the hole diameter or, in an inverse way, change to the mandrel diameter can cause a significant change in the residual stress field.

This requirement on mandrel and sleeve specification severely limited the number of academic papers that could be used to make comparisons.

The area perpendicular to the direction of load is the most important for making estimations on the fatigue resistance of a component. In this work, stresses were examined parallel to the direction of load but because a split sleeve was not used, there is very little difference in the residual stress field close to the hole. To compare directly with the literature, stresses were examined in the *y-z* plane instead of the *x-z* plane used for taking measurements in the results, section 6. The coordinate system and the cross-section of interest are shown in Figure 7.2.

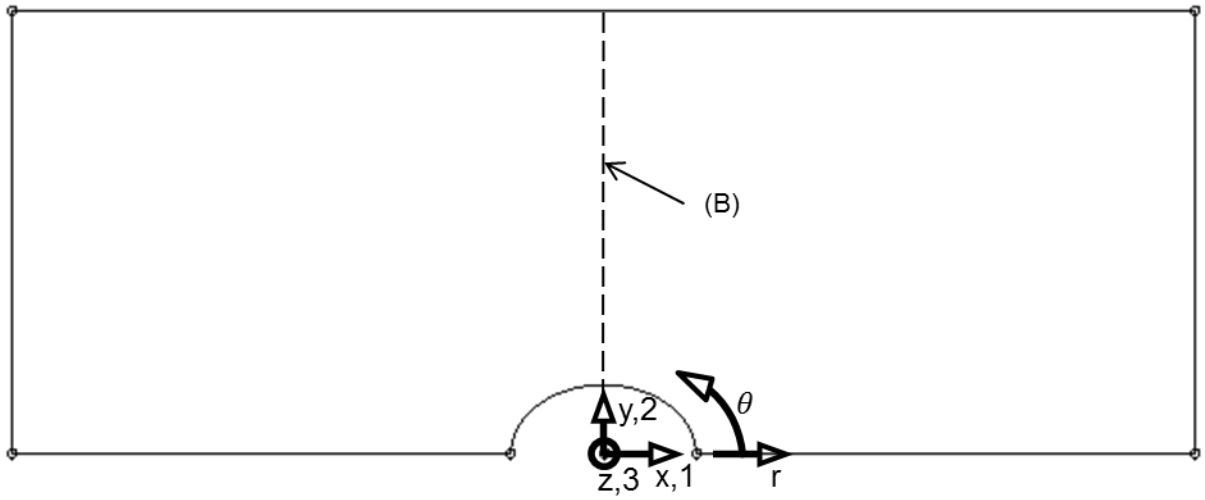


Figure 7.2: Coordinate system illustrating the plane along which measurements were made for literature comparison (B).

The first paper considered was written by S.J. Houghton and S.K. Campbell, [Houghton, 2011]. This paper used a quarter plate model to analyze the effect of friction, inclusion and exclusion of the sleeve, and different strain hardening rules. The Houghton results used for comparison included a sleeve and use kinematic hardening, Figure 7.3. These were compared directly to the results for a model generated in this study at the entrance, middle, and exit surfaces of the plate. When the model from this study, in solid black line, is compared to the results for kinematic hardening, dark blue line with blue squares, at the middle surface, they match fairly well. The results from entrance and exit surfaces show greater variation. It has been known that the free surfaces are the most difficult to accurately predict. Due to the high rate of change in the stresses at the entrance and exit surfaces, the data at a point just beneath the surface

was also compared, shown in neon blue. It is interesting to note that when compared to the reported finding the model data just below the surface is a very close match.

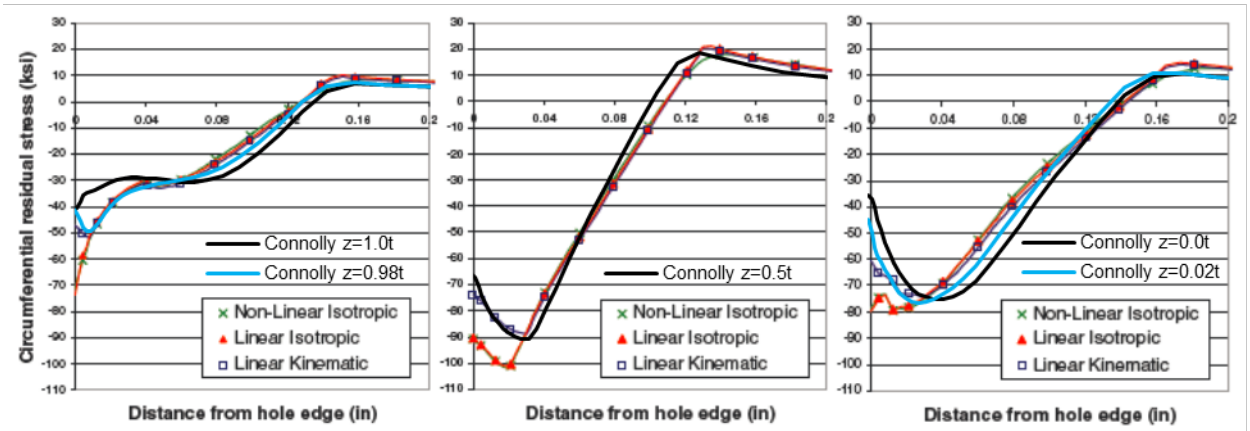


Figure 7.3: Comparison of generated data based to the Houghton paper at the entrance (left), middle (center), and exit (right) surfaces.

Another paper used for comparison was written by Ismonov et. al, [Ismonov 2009a]. This work focused on the effects of friction, kinematic versus isotropic hardening, and inclusion of a split in the sleeve. This paper had both a finite element model and results from actual test cases. To obtain data from test coupons, displacement measurements were taken to obtain stresses using the contour method at the entrance, exit, and mid surfaces. The Ismonov paper is a bit different from the Houghton work and the work done here, in that the Ismonov paper the hole is reamed after the expansion process. Because the work here does not ream the finite element model, the results are shifted so their position matches if compared to the hole center. After making these shifts, it is found that that the results generated using the generated model match fairly well to the finite element results given in the paper. This model was relatively thin so the difference is small between the free surface and 2% of the thickness away from the surface. The major difference between the generated model and the paper results are at the point of maximum tension. The generated model indicates that the point of maximum tension would be closer to the hole, this is possibly due to the lower mesh resolution away from the hole or the coordinate shift used to take reaming into account.

A comparison of finite element results to measurements taken from the experimental coupon shows they are consistent. Differences between measured and predicted values are most

noticeable at the plate edges, where it is known that the contour method has difficulty making accurate measurements.

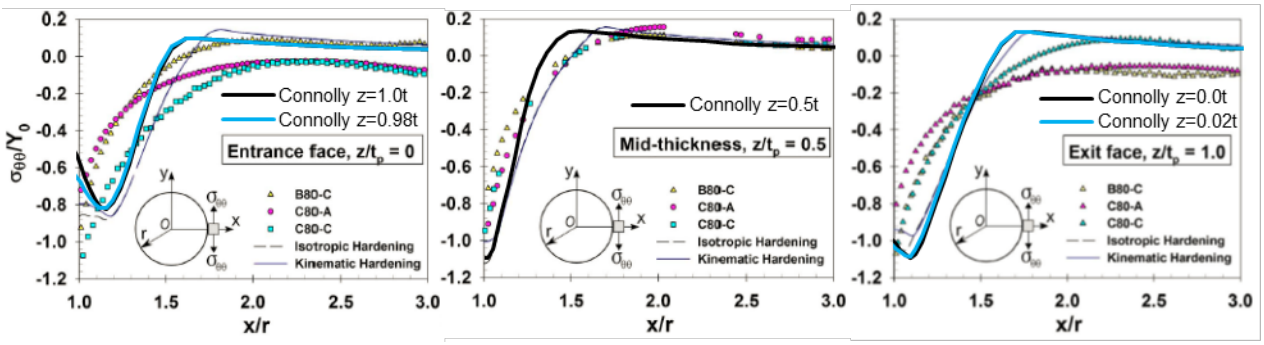


Figure 7.4: Comparison of generated data based on the Ismonov paper at the entrance (left), middle (center), and exit (right) surfaces.

## 7.2 Lessons Learned

An early goal of this project was to create a Python script capable of generating Abaqus input to test cold expansion with a variety of geometries and model conditions. While the script can generate a wide range of models, certain selections make the model unstable and unable to run to completion. The exact reason for the instabilities was not determined during this work.

While some options would sporadically function correctly, a number of options consistently caused the model to become non-convergent. If the sleeve used in the expansion was split, some versions of the model would not run while others did. Those that failed did so when the mandrel's maximum thickness was near the exit surface. After trying a range of materials for literature comparison and curiosity, it was found that a drastic increase in the stiffness would also cause problems. A model containing aluminum plate(s) and a straight sleeve would run well; however, if a stiffer material like steel is used, the contact method cannot resolve the interaction between the sleeve and the hole in the plate(s). According to the FTI regulations a flared sleeve is supposed to be used when the hole does not contain a counter-sink. The addition of a flared sleeve that was not split would cause the model to fail almost immediately after components began making contact. It is possible that the flared sleeve behaves more stiffly than the straight sleeve and this causes the model to be non-convergent. In some cases, the inclusion of friction caused the model to run better but it was never obvious why. Many of the instabilities registered as problems in the calculation of contact. As such, many of the solutions to make models convergent involved slightly modifying the specifics of the contact property. It was difficult to

determine if the underlying problem was the contact itself or if other issues were simply expressing themselves by causing the contact between components to be problematic.

Many variations were initially considered for analysis but due to time restrictions the number was reduced. When reducing the number of model parameters, the reliability of the configuration as well as whether or not it has been studied previously were taken into account. Due to a change in software to a newer version, mesh refinement, and changes in contact properties, a number of variations that had initially worked became non-convergent. Because the genesis of the project was to study the effect of simultaneous multi-plate expansion, great lengths were taken to make sure this type of model would run properly.

The inclusion of the counter-sink and extended boundary conditions were only used for a single model due to difficulties in making counter-sink models that ran to completion. This model was incorporated in the analysis to show that including the counter-sink was possible, and this produced results in line with other two-plate models, Figure 7.5. It also helped to illustrate the importance in location of the boundary conditions.

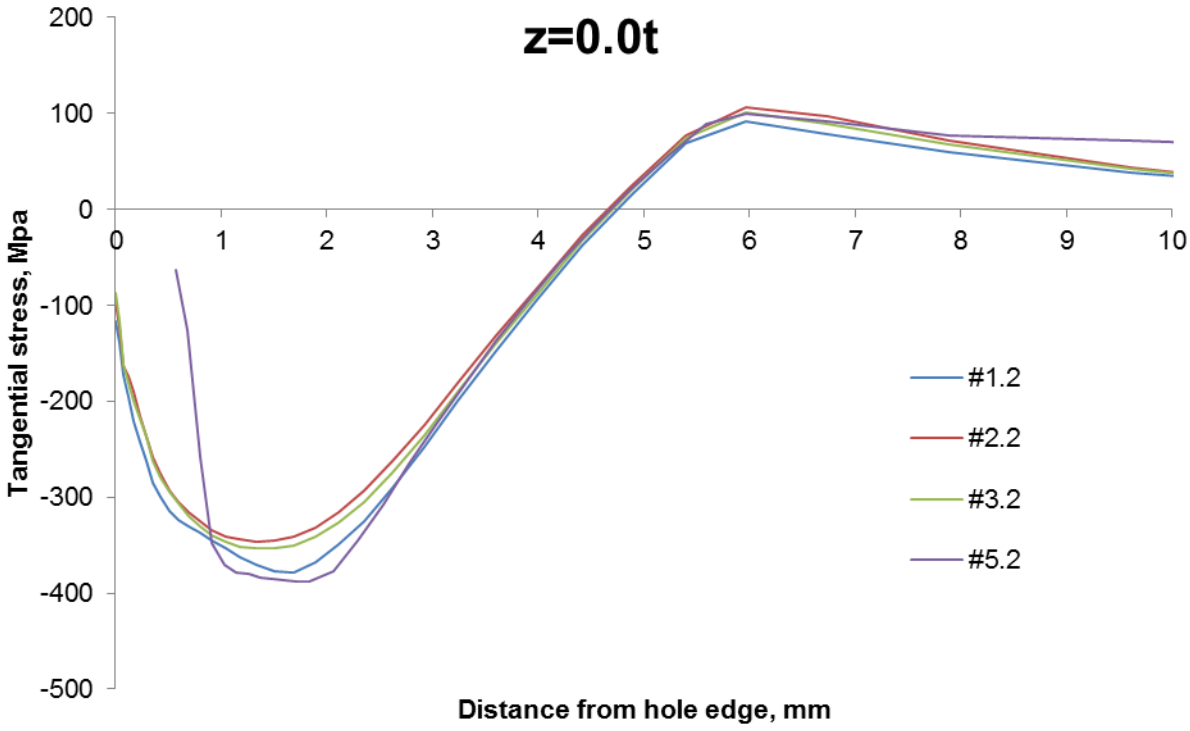


Figure 7.5: Tangential stress at the exit surface of the lower plates from two-plate expansions, one with a counter-sink #5.2.

One of the major points that can be taken away from this work is that there can be inherent difficulties with creating an overly versatile model. The changing of aspects in the model by addition, subtraction, or modification of components can result with instability. This does not mean that a single script cannot be used to generate a number of different model types, but rather that it is not guaranteed that models will run to completion on the first attempt. It is likely that with enough time the correct parameters could be modified to make models convergent, however, this process may be required any time a new set of parameters are chosen together for analysis.

## 7.3 Future Improvements

There are many possibilities for how this script generated model may be used to research cold expansion. Even though it may be difficult to get complex models to run to completion, this does not preclude the possibility that with the proper modifications any model could be made convergent. Some of the model variations mentioned above have already been discussed in other papers, specifically friction, split compared closed sleeve, and some variations in the material properties. Future work could include the aspects mentioned above along with others.

In addition to implementing the previously mentioned aspects, there is also interest in expanding the capabilities of the script. One point of interest for investigation is the effect of hole proximity to the edge of the plate. This could be done by simple modification of where on the half plate model the fixed and free edges are defined. By swapping the fixed and free conditions, the plate is essentially turned 90 degrees, making it possible to change the position of the hole with respect to the free edge. This set up would not apply to including the split sleeve, because the symmetry condition is no longer in line to let the split occur properly.

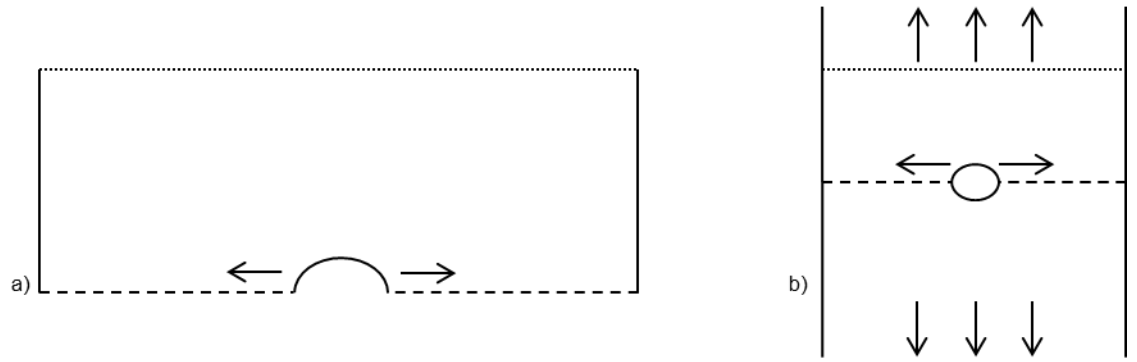


Figure 7.6: (a) 2D representation of boundary conditions, symmetry condition shown using dashes and fixed condition using dots, (b) illustration of modeled section with respect to component.

As these are fastener holes being studied, it makes sense to examine the effect of bolts with the two-plate models. By adding a bolt and displacement conditions to the hole, it would be possible to simulate the insertion and tightening of a bolt. This could be used to determine what the stress field looks like during the operation of the component. In a similar way, this kind of technique could be used to examine the effect of interference bolting on the residual stress field. An interference bolt is one that is slightly larger than the hole it is placed in, which is done to change the stress field in the region of the hole. Counter-sink holes are also a fairly common occurrence in industry, making further investigation of this geometry a potentially useful tool.

## 7.4 Application to Field Work

Even with the difficulties mentioned above, some statements can be made about situations not specifically tested in this work, which could have bearing on cold expansion in the field. It can be surmised that two-plate interactions will behave in a similar fashion with multiple plates or stiffer plates. When dealing with aluminum, the multi-plate effects that occur at the interface should be consistent with what has already been shown for the two-plate model. It is expected that entrance and exit effects will be the same regardless of the number of plates in the stack-up. Similar effects are also expected if plates of higher stiffness are included. Through the work done on this project and results discussed previously, it is possible to make comments on how different methods may be used to improve the practical use of cold expansion. It is also possible to make useful insight into the monitoring and implementation of cold expansion.

### 7.4.1 Strain Monitoring

The strain analysis from the model has shown a definitive link between the edge of the plastic region and the point of maximum tension. This behavior could be a used as an alternative method for determining if cold working has been performed properly. Current methods for analyzing cold expansion in the field use X-ray diffraction to directly measure the surface residual stresses around a cold expanded hole. This equipment is cumbersome and can be dangerous. However, if the size of the plastic zone at the surface can be measured during or after the cold expansion process, then it may be used to infer that a proper residual stress field is present. While these methods may be just as cumbersome as X-ray diffraction, there could be some which prove easier to implement.

### 7.4.2 Boundary Clamping

Even though only one model included the extensions to adjust clamping, it demonstrated some obvious differences in the results. Clamping conditions are a reality of field work that has not been studied in depth. Layer clamping in the field can vary significantly depending on the part that is being cold expanded. In most cases, clamping is not actively applied, rather, the surrounding components, e.g., bolts in adjacent holes, provide the clamping condition. This leaves a large variance in how close the clamping is to the hole and could affect the residual stress field as shown in the results presented earlier, section 6.3.

### 7.4.3 Sacrificial Top Plate

It has been shown that some out-of-plane displacement occurs at the hole's entrance and exit as a result of cold expansion. At the interface of the plates, these out of plane displacements interact, changing the residual stress field that is produced. The entrance surface of a plate that is located at an interface receives additional benefits from the cold expansion process that it would not otherwise receive if the surface was completely free during the expansion. This leads to the possibility of using an additional piece of material to create an interface where there normally would not be one, for the sole purpose of enhancing the residual stress field at a plate's entrance surface. This plate would obviously be deformed by the cold expansion process, so a single hole in this sacrificial plate could only be used once, unless it was reamed to function with a larger hole expansion. If a sacrificial plate was used at the entrance of a stack-up, it would mean that all

plate entrance surfaces would receive the additional compressive benefit. Practical application of this method would require access to the entrance side of a stack-up which would not be possible if the surface was unreachable, such as the interior of a plane wing.

### 7.4.4 Difficulties of Combine Steel and Aluminum Stack-up

Even though it was not successfully tested, conjecture can be made about the effect of cold expansion in stack-ups that include two materials of radically different stiffness. While different toolsets exist for different classes of material, aluminum and mild steel, versus titanium and high strength steel, it is not always practical to separate plates before cold expansion. Assuming that holes in this stack up need to finish at the same diameter, a decision needs to be made on which toolset to use. In most cases, the lower stiffness toolset is too wide to be used on a hard plate with the same starting hole diameter as a softer plate. This could lead to the idea that the toolset intended for higher stiffness should be used in these circumstances. It is important to note that the diameter of the higher stiffness toolset is smaller than the minimum diameter for expansion in the toolset for the less stiff material. So, while this arrangement will cause the proper expansion for the harder material, the softer material will be under expanded by a large margin. This under-expansion in an already weaker material could be undesirable. As shown in section 6.2, a lower degree of interference between mandrel and plate can cause peak compressive stress to occur closer to the hole edge. It is not clear whether moving the max compressive stress closer to the hole will have a beneficial or detrimental effect on the fatigue life of a component. A brief analysis was attempted to compare the residual stress field of an aluminum plate expanded using both toolsets. However, there was not enough time to diagnose an apparent discrepancy noted in the results, so no conclusion was reached.

It seems probable that there is a combination of different starting hole sizes where simultaneous expansion and final reaming would yield acceptable results. This technique could be applicable for components at manufacture but not in the field. Once in operation, drilling the holes to different diameters would require disassembly, at which point single plate cold expansion would be feasible. This technique may also be problematic because the touching surfaces are at different diameters and may cause unanticipated effects.

# 8 Conclusions

Cold expansion is an increasingly common process used in a number of different industries to enhance the fatigue resistance of components containing fastener holes. While different methods for cold expansion have been developed, one of the most common is the processes of slip sleeve cold expansion developed by FTI. The principles of cold expansion are well understood. By creating a compressive residual stress field around the hole, stresses in this region are effectively reduced during operation, thus extending the fatigue life of the component. In order to improve the life estimations for cold expanded holes, detailed knowledge of the residual stress field is required. Making life estimations for these components is difficult due to the three-dimensional and complex nature of the residual stress field generated by cold expansion. Many different methods and models have been used to try to predict this stress field, each with its own benefits and simplifications. Due to the nature of cold expansion, it is most accurately captured by modeling the process using a three-dimensional finite element code. Different aspects of the cold expansion process have been analyzed in a number of academic papers, including friction, different material models, temperature effects, and cyclic effects.

The motivation of this project was the creation of a model generating script, which could be used to create a number of different cold expansion cases. Models generated by this script were intended to run on a personal machine and were therefore kept to as few elements as possible while maintaining accuracy. The script was then used to create models that explored different factors present in the cold expansion process. This work focused on exploring how changes in interference can affect the residual stress fields produced. Two sets of models were considered when observing interference effects. First was the effect of varying the hole size and the second was the implications of a simultaneous two-plate expansion.

It was found that increasing the starting size of a hole while maintaining the same dimensions for the mandrel had a number of effects. If the starting hole size is increased past a critical point, there is a radical drop off in the size of the compressive zone created by the cold expansion process. Up to this critical point a number of trends were seen. As the hole size is increased, the point of maximum compression remains fairly constant in stress, but its position moves closer to hole edge. Additionally, as the hole size increases, the point of maximum tension decreases in magnitude and also moves closer to the bore of the hole. Decreasing the hole size to

a point smaller than the minimum recommended was not analyzed in this work. This decrease in hole size would most likely lead to damage at the hole surface that cannot be captured using this finite element model.

By creating a two-plate simultaneous expansion, surfaces that were once free at the entrance and exit of a plate become partially constrained. This change in boundary condition has a definite effect on the residual stress field near the interface of the two-plates. In these two-plate models the interface is formed at the exit surface of the first (top) plate to experience expansion and the entrance surface of the second (bottom) plate. Very little effect was found away from these previously free surfaces. At the interface, both plates showed an increase in the compressive residual stress field close to the hole. This localized effect dropped off a small distance away from the hole edge. The benefit seen at the exit surface of the top plate was relatively small, though noticeable. At the entrance surface of the bottom plate, the improvement in the compressive stress field is more pronounced. In the small region at the surface near the hole edge, the tangential residual stress was almost twice as compressive as its free surface counterpart. This increase in the compressive residual stress field is thought to be the result of hydrostatic stresses introduced at the surface by the interference of the two-plates.

The model went through a number of variations to arrive at a “baseline” model with suitable accuracy at the free surfaces while containing as few elements as possible. Due to the unique nature of this work, there are no direct comparisons within the literature. Physical samples were unavailable to test, so the script was used to generate models that mirrored the conditions found in academic papers. Two papers were found with the necessary specifications given to recreate their test specimens. Analyses done in this work for comparison purposes were found to be in line with those shown by these other authors.

This work has shown a number of interesting concepts that can be used to improve the practice of cold expansion. Most notable of these is the idea of intentionally creating a multi-layer stack up to produce better surface results at the entrance face of a plate. This concept has not been presented before, as this is the first finite element work to show the benefits of multi-layer cold expansion. Multi-layer modeling has also shown that changing the clamping conditions in a stack-up can impact the subsequent residual stress field. This is an important

aspect to consider when performing cold expansion in the field, where boundary clamping may not be well controlled.

The flexibility of this script generated model has the potential for additional study into the characteristics that affect residual stress fields produced by cold expansion. With enough time and expertise, a number of other model variations could be implemented in addition to those already shown. While there are many possibilities for using this kind of script generated modeling, it may take some time to ensure that every set of model parameters continues to produce convergent models.

# 9 Bibliography


Amrouche, 2003 — Amrouche, A., Mesmacque, G., Garcia, S., Talha, A., "Cold expansion effect on the initiation and the propagation of the fatigue crack", *International Journal of Fatigue*, Vo. 25, pp. 949-954, 2003.

Ball, 2003 — Ball, D.L, Doerfler, M.T., "Experimental and analytical studies of residual stress field evolution and fatigue crack growth at cold expanded holes", 2003 USAF ASIP Conference, Savannah GA, 2003.

Callinan, 2010 — Callinan, R.J., Kaye, R., Meller, M., "Investigation of stress intensity factor for overloaded holes and cold expanded holes", 6th Australasian Congress on Applied Mechanics, Perth Australia, 2010

Chakherlou, 2003 — Chakherlou, T.N., Vogwell, J., "The effect of cold expansion on improving the fatigue life of fastener holes", *Engineering Failure Analysis*, Vol. 10, pp. 13-24, 2003.

Chakherlou, 2011 — Chakherlou, T.N., Alvandi-Tabrizi, Y., Kiani, A., "On the fatigue behavior of cold expanded fastener holes subjected to bolt tightening", *International Journal of Fatigue*, Vol. 33, pp. 800-810, 2011.

Chakherlou, 2012 — Chakherlou, T.N., Shakouri, M., Aghdam, A.B., Akbari, "Effect of cold expansion on the fatigue life of Al 2024-T3 in double shear lap joints: Experimental and numerical investigations", *Material and Deisgn*, Vol. 33, pp. 185-196, 2012.

Clark, 2003 — Clark, D.A., Johnson, W.S., "Temperature effects on fatigue performance of cold expanded holes in 7050-T7451 aluminum alloy", *International Journal of Fatigue*, Vol. 25, pp. 159-165, 2003.

Cook, 1989 — Cook, R., "The United Kingdom contribution to the AGARD 'Fatigue-rated fastener systems' programme", *Royal Aerospace Establishment Technical Report 89046*, 1989.

de Matos, 2007 — de Matos, P.F.P., McEvily, A.J., Moreira, P.M.G.P., de Castro, P.M.S.T., "Analysis of the effect of cold-working of rivet holes on the fatigue life of an aluminum alloy", *International Journal of Fatigue*, Vol. 29, pp. 575-586, 2007.

Dowling, 2013 — Dowling, N.E., *Mechanical Behavior of Materials: Engineering Methods for Deformation, Fracture, and Fatigue*, 4th edition, Pearson Prentice Hall, Upper Saddle River, NJ, 2013.

Finney, 1995 — Finney, J.M., Evans, R.L., "Extending the fatigue life of multi-layer metal joints", *Fatigue Fracture Engineering Material Structures*, Vol. 18, No. 11, pp. 1231-1247, 1995.

FTI, 2011 — Fatigue Technology Inc. www.fatiguetech.com, "Cold Expansion of Holes Using the Standard Split Sleeve System and Countersink Cold Expansion", *FTI Process Specification 8101* Revision G, 2011.

| | |
|---|---|
| Garcia, 2005 | Garcia, S., Amrouche, A., Mesmacque, G., Decoopman, X., Rubio, C., "Fatigue damage accumulation of cold expanded hole in aluminum alloys subjected to block loading", *International Journal of Fatigue*, Vol. 27, pp. 1347-1353, 2005. |
| Garcia-Granada, 1999 | Garcia-Granada, A.A., Lacarac, V., Smith, D.J., Pavier, M.J., Cook, R., Holdway, P., "3D residual stresses around cold expanded holes in a new creep resistant aluminium alloy", *Transactions on Engineering Sciences*, Vol. 25, 1999. |
| Garcia-Granada, 2001 | Garcia-Granada, A.A., Lacarac, V., Smith, D.J., Pavier, M.J., "A new procedure based on Sachs' boring for measuring non-axisymmetric residual stresses: experimental application", *International Journal of Mechanical Sciences*, Vol. 43, pp. 2753-2768, 2001. |
| Houghton, 2011 | Houghton, S.J., Campbell, S.K., "Identifying the residual stress field developed by hole cold expansion using finite element analysis", *Fatigue & Fracture of Engineering Materials & Structures*, Vol. 35, pp. 74-83, 2011 |
| Ismonov, 2009a | Ismonov, S., Daniewicz, S.R., Newman Jr., J.C., Hill, M.R., Urban, M.R., "Three Dimensional Finite Element Analysis of a Split-Sleeve Cold Expansion Process", *Journal of Engineering Materials and Technology*, Vol. 131, 2009. |
| Ismonov, 2009b | Ismonov, S., Daniewicz, S.R., Newman Jr., J.C., "Elastic-Plastic Stress Analysis of Cold-Worked Pin-Loaded Holes", *Journal of ASTM International*, Vol. 6, No. 10, 2009. |
| Lacarac, 2000 | Lacarac, V., Smith, D.J., Pavier, M.J., Priest, M., "Fatigue crack growth from plain and cold expanded holes in aluminium alloys", *International Journal of Fatigue*, Vol. 22, pp. 189-203, 2000. |
| Lacarac, 2001 | Lacarac, V., Smith, D.J., Pavier, M.J., "The effect of cold expansion on fatigue crack growth from open holes at room and high temperature", *International Journal of Fatigue*, Vol. 23, pp. 5161-5170, 2001. |
| Lacarac, 2004 | Lacarac, V.D., Garcia-Granada, A.A., Smith, D.J., Pavier, M.J., "Prediction of the growth rate for fatigue cracks emanating from cold expanded holes", *International Journal of Fatigue*, Vol. 26, pp. 585-595, 2004. |
| Mahendra Babu, 2008 | Mahendra Babu, N.C., Jagadish, T., Ramachandra, K., Sridhara, S.N., "A simplified 3-D finite element simulation of cold expansion of a circular hole to capture through thickness variation of residual stresses", *Engineering Failure Analysis*, Vol.15, pp.339-348, 2008. |
| Noyan, 1987 | Noyan, I.C., Cohen, J.B., *Residual stress: measurement by diffraction and interpretation*, Springer-Verlag, New York, NY, 1987. |
| Pavier, 1998 | Pavier, M.J., Ponssard, C.G.C., Smith, D.J., "Finite element modeling of the interaction of residual stress with mechanical load for a crack emanating from a cold worked fastener hole", *Journal of Strain Analysis* |

*for Engineering Design* Vol. 33, No. 4, pp. 275-289, 1998.

Prevey, 1986 — Prevey, P.S., "X-Ray Diffraction residual stress techniques", Metals Handbook 10th ed., Metals Park: American Society for Metals, pp. 380-392, 1986

Reese, 2009 — Reese, E.D., Dowson, A.L., Jones, T.G.B., "The Variable Expansion Process – A New Cost Efficient Method for Cold Working Fastener Holes in Aluminum Aircraft Structures", 25th ICAF Symposium – Rotterdam, 2009.

Reid, 2001 — Reid, L., "Sustaining an Aging Aircraft Fleet with Practical Life Enhancement Methods", *RTO AVT Specialists' Meeting on "Life Management Techniques for Ageing Air Vehicles"*-Manchester, 2001.

Smith, 1986 — Smith, R.A., "Thirty Years of Fatigue Crack Growth--an Historical Review", Proceedings of a Conference on Fatigue Crack Growth, Cambridge, 1986.

Stefanescu, 2003 — Stefanescu, D., Edwards, L., Fitzpatrick, M.E., "Stress intensity factor correction for asymmetric through-thickness fatigue cracks at holes", *International Journal of Fatigue*, Vol.25, pp.569-576, 2003.

Tiffany, 2010 — Tiffany, C. F., Gallagher, J. P., Babish IV, C. A., "Threats to aircraft structural safety, including a compendium of selected structural accidents/incidents", *Engineering Directorate (ASC/EN) Aeronautical Systems Center*, March Final Report, 2010.

Toor, 1976 — Toor, P.M., "Cracks emanating from precracked coldworked holes", *Engineering Fracture Mechanics*, Vol. 8, pp.391-395, 1976.

Zhang, 2003 — Zhang, X., Wang, Z., "Fatigue life improvement in fatigue-aged fastener holes using the cold expansion technique", *International Journal of Fatigue*, Vol. 25, pp. 1249-1257, 2003.